Reconfigurable Intelligent Surface for Green Edge Inference

Sheng Hua, *Student Member, IEEE,* Yong Zhou, *Member, IEEE,* Kai Yang, *Student Member, IEEE,*
and Yuanming Shi, *Member, IEEE*

arXiv:1912.00820v2 [eess.SP] 5 Dec 2019

Abstract—Reconfigurable intelligent surface (RIS) as an emerging cost-effective technology can enhance the spectrum- and energy-efficiency of wireless networks. In this paper, we consider an RIS-aided green edge inference system, where the inference tasks generated from resource-limited mobile devices (MDs) are uploaded to and cooperatively performed at multiple resource-enhanced base stations (BSs). Taking into account both the computation and uplink/downlink transmit power consumption, we formulate an overall network power consumption minimization problem, which calls for the joint design of the set of tasks performed by each BS, transmit and receive beamforming vectors of the BSs, transmit power of the MDs, and uplink/downlink phase-shift matrices at the RIS. Such a problem is a mixed combinatorial optimization problem with nonconvex constraints and is highly intractable. To address the challenge of the combinatorial objective, a group sparse reformulation is proposed by exploiting the group sparsity structure of the beamforming vectors, while a block-structured optimization (BSO) approach is proposed to decouple the optimization variables. Finally, we propose a BSO with mixed $\ell_{1,2}$-norm and difference-of-convex-functions (DC) based three-stage framework to solve the problem, where the mixed $\ell_{1,2}$-norm is adopted to induce the group sparsity of beamforming vectors and DC is adopted to effectively handle the nonconvex rank-one constraint after matrix lifting. Numerical results demonstrate the supreme gain of deploying a RIS and confirm the effectiveness of the proposed algorithm over the baseline algorithms.

Index Terms—Reconfigurable intelligent surface, joint uplink and downlink, green edge inference, block-structured optimization, mixed $\ell_{1,2}$-norm, difference-of-convex programming

I. INTRODUCTION

Benefiting from the availability of big data, recent years have witnessed the rapid prosperity of deep neural network (DNN), which has demonstrated its superiority in a variety of intelligent applications (e.g., computer vision and natural language processing). Meanwhile, with an ever-increasing number of mobile devices (MDs) that will generate 77 exabytes data per month by 2022 [2], the demand of performing inference tasks (e.g., object recognition and machine translation) is anticipated to be ubiquitous, especially in the artificial intelligence (AI)-powered sixth generation (6G) networks [3].

Driven by this trend, it is urgent to push traditional cloud-based DNN models to the network edge so as to unleash the potentials of edge data and in turn provide intelligent services [4]-[5]. One possible architecture to perform inference tasks is on-device inference, i.e., running DNN models directly on MDs. While the model compression [6], model selection [7], and hardware acceleration [8] have been proposed as promising techniques to help MDs run DNN models, deploying powerful models with real-time execution requirements is still challenging because of the resource limitations of MDs [4].

By leveraging edge computing [9] and deploying DNN models at the edge base stations (BSs) that have strong computational capacity and large storage resources, edge inference stands out as a promising paradigm to provide intelligent services for MDs [10]. To accomplish the inference tasks, the MDs upload the task-specific data to the BSs and subsequently the BSs deliver the inference results after finishing the inference process. Tailored for latency-critical applications, the authors proposed device-edge [11] and edge-cloud [12] synergy frameworks to partition DNN model parameters based on network dynamics so as to minimize the execution latency. As energy efficiency is a key performance indicator for edge inference systems [10], the authors in [13]-[14] proposed energy-aware approaches to prune DNN models so as to minimize the computation power consumption (i.e., power required for the BSs to perform the inference tasks) while maintaining reasonable inference precision. However, the communication power consumption is not considered in [13]-[14]. The authors in [15] proposed to minimize the sum of computation power and downlink transmit power consumption (i.e., power required for the BSs to deliver the tasks results to the MDs), while the uplink transmit power (i.e., power required for the MDs to upload data to the BSs) is neglected. However, the uplink traffic load (e.g., raw images for an object recognition task) is usually comparable to the downlink one (e.g., labeled images) in edge inference systems, resulting in high uplink transmit power consumption. Therefore, it is imperative to develop new techniques to reduce both the uplink and downlink transmit power consumption and in turn facilitate an energy-efficient design for edge inference systems.

Recently, a growing line of works focused on an emerging technology named reconfigurable intelligent surface (RIS [16], or reconfigurable meta-surface [17], hypersurface [18]), which has the potential to significantly reduce the power consumption [19] and improve the energy efficiency [20]. An RIS is a low-cost planar array consisting of a large number of passive

S. Hua, Y. Zhou, and Y. Shi are with the School of Information Science and Technology, ShanghaiTech University, Shanghai 201210, China (E-mail:{huasheng, zhouyong, shiym}@shanghaitech.edu.cn).

K. Yang is with the School of Information Science and Technology, ShanghaiTech University, Shanghai 201210, China, also with the Shanghai Institute of Microsystem and Information Technology, Chinese Academy of Sciences, Shanghai 200050, China, and also with the University of Chinese Academy of Sciences, Beijing 100049, China (E-mail: yangkai@shanghaitech.edu.cn).

reflecting elements with reconfigurable phase shifts, each of which can be dynamically tuned via a software controller to reflect the incident signals [21]-[22]. These elements consume negligible energy due to their passive nature. By adaptively adjusting the phase shifts of reflecting elements, an RIS can combine the constructive signals and suppress the interference, thereby greatly enhancing the performance of wireless systems [17]-[18]. By jointly optimizing the beamforming vectors and the phase-shift matrix, deploying an RIS has been shown as an effective way to reduce the power consumption in various applications, e.g., downlink unicast [19] and broadcast [23] settings, non-orthogonal multiple access [24]-[25], and simultaneous wireless information and power transfer [26]. All the previous works only considered the downlink transmit power consumed by the BSs. However, in edge inference systems, the computation power consumption is an indispensible component and should be taken into account to accurately characterize the overall network power consumption. In addition, it is essential to optimize both the uplink and downlink phase-shift matrices of the RIS to assist both the uplink and downlink data transmissions. These two key issues make the approaches proposed in the existing works not applicable to our work.

To guarantee the quality of intelligent services provided for MDs, we explore the idea of computation replication [27], which allows inference tasks to be performed by multiple BSs to create multiple copies of the inference results at different BSs. These copies enable cooperative downlink transmission among the BSs on delivering inference results. In terms of power consumption, however, cooperative transmission and computation replication conflict with each other. Specifically, cooperative transmission reduces downlink transmit power consumption by exploiting a higher beamforming gain, while computation replication rapidly increases the computation power consumption because of repeatedly running DNN models for multiple times. Therefore, we should strike a balance between the computation and communication power consumption via selecting inference tasks performed by each BS and in turn achieve green edge inference.

In this paper, we consider an RIS-aided green edge inference system with multiple BSs cooperatively performing inference tasks for multiple MDs, taking into account both uplink and downlink transmit power consumption as well as the computation power consumption. Our objective is to minimize the overall network power consumption subject to prescribed quality-of-service (QoS) requirements, by jointly designing the task selection strategy, transmit/receive beamforming vectors of the BSs, the transmit power of the MDs, and the uplink/downlink phase-shift matrices at the RIS. However, the formulated problem is a mixed combinatorial optimization problem with nonconvex constraints, which is highly intractable.

A. Contributions

The main contributions of this paper are summarized as follows.

- We propose a joint design of the task selection strategy, transmit/receive beamforming vectors, transmit power, and uplink/downlink phase-shift matrices for an RIS-aided

green edge inference system. To the best of our knowledge, this is the first attempt to unify beamforming vectors, transmit power, and phase shifts design in both the uplink and downlink transmissions into a general framework.
- The combinatorial nature of the task selection strategy and the coupled optimization variables stand out as two major challenges. We address the challenge of the combinatorial variable by exploiting the group sparsity structure of the beamforming vectors, and tackle the challenge of the coupled variables by proposing a block-structured optimization (BSO) approach.
- With fixed phase shifts, we adopt the weighted mixed $\ell_{1,2}$-norm to induce the group sparsity of beamforming vectors. With fixed beamforming vectors and transmit power, the original problem is transformed to a homogeneous quadratically constrained quadratic programming (QCQP) with a nonconvex rank-one constraint. As the widely adopted semidefinite relaxation (SDR) technique incurs performance degradation when the number of reflecting elements is large, we propose a novel difference-of-convex-functions (DC) representation for this nonconvex constraint, followed by proposing an effective DC algorithm. We then propose a BSO with mixed $\ell_{1,2}$-norm and DC based three-stage framework to solve the original problem.
- Through extensive simulations, we show that the deployment of an RIS can significantly reduce the overall network power consumption. Furthermore, the proposed BSO with mixed $\ell_{1,2}$-norm and DC algorithm achieves a significant performance improvement compared to BSO with mixed $\ell_{1,2}$-norm and SDR algorithm, which demonstrates the effectiveness of DC in yielding the rank-one solutions.

B. Organization and Notations

Organization: The remainder of this paper is organized as follows. We present the system model and problem formulation in Section II. A BSO approach is developed in Section III. Based on mixed $\ell_{1,2}$-norm and DC approach, we propose a three-stage framework in Section IV. Simulation results are illustrated in Section V. Finally, Section VI concludes this paper.

Notations: We use boldface lower-case (e.g., $\boldsymbol{h}$) and upper-case letters (e.g., $\boldsymbol{G}$) to represent vectors and matrices, respectively. The transpose, conjugate transpose, trace operator and diagonal matrix are denoted as $(\cdot)^\mathsf{T}, (\cdot)^\mathsf{H}, \mathrm{Tr}(\cdot)$ and $\mathrm{diag}(\cdot)$, repectively. The symbols $|\cdot|$ and $\Re(\cdot)$ denote the modulus and the real component of a complex number. The $n \times n$ identity matrix is denoted as $\boldsymbol{I}_n$. The complex normal distribution is denoted as $\mathcal{CN}$. The inner product of two matrices $\boldsymbol{X}$ and $\boldsymbol{Y}$ is denoted as $\langle \boldsymbol{X}, \boldsymbol{Y} \rangle$, which is defined as $\langle \boldsymbol{X}, \boldsymbol{Y} \rangle = \mathrm{Tr}(\boldsymbol{X}^\mathsf{H}\boldsymbol{Y})$. The ℓ_2-norm of a vector is denoted as $\|\cdot\|_2$. The spectral norm and Frobenius norm of a matrix are denoted as $\|\cdot\|$ and $\|\cdot\|_F$, respectively. The i-th largest singular value of matrix $\boldsymbol{X}$ is denoted as $\sigma_i(\boldsymbol{X})$. We use $\mathbf{1}_{\{\cdot\}}$ to denote the indicator function which outputs 1 if the condition $\cdot$ is satisfied, and outputs 0 otherwise. In the rest of this paper, the superscripts UL and DL refer to uplink and downlink, respectively, and the
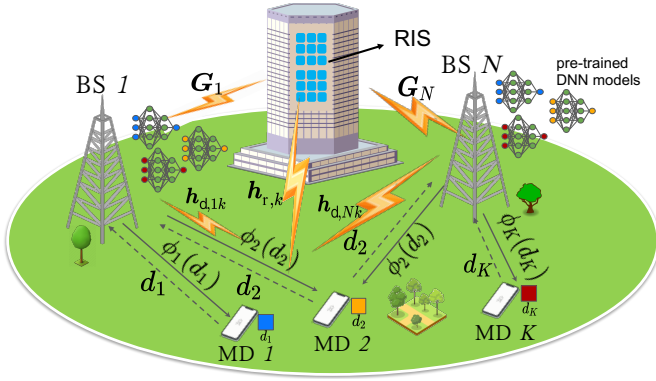
Fig. 1: A reconfigurable intelligent surface (RIS)-aided edge inference system with N base stations (BSs) collaboratively serving K mobile devices (MDs). The RIS is deployed on the facade of a building.

letters d and r in the subscripts stand for the *direct link* and the *reflected link*, respectively.

II. SYSTEM MODEL AND PROBLEM FORMULATION

In this section, we describe the system model and the power consumption model for performing inference tasks at the network edge, followed by an overall network power minimization formulation for green edge inference while guaranteeing the quality of intelligent services.

A. System Model

We consider an RIS-aided edge computing system, where N L_n-antenna BSs distributed in a small-cell network collaboratively serve K single-antenna MDs with the assistance of an M-element RIS deployed on the facade of a building, as shown in Fig. 1. Let $\mathcal{N} = \{1, \ldots, N\}$, $\mathcal{K} = \{1, \ldots, K\}$, and $\mathcal{M} = \{1, \ldots, M\}$ denote the index sets of BSs, MDs, and reflecting elements, respectively. The BSs are resource-enhanced with strong computation and storage capabilities [28]. Each MD has an inference task (e.g., image recognition) to be processed by a task-specific DNN model (e.g., AlexNet [29]). Specifically, the DNN model denoted as ϕ_k takes MD k's local data d_k (e.g., raw images) as input and generates the inference result $\phi_k(d_k)$ (e.g., labeled images) as output. As it is infeasible to run DNN models on resource-constrained MDs, we in this paper propose to perform inference tasks for the MDs at the BSs. We assume that all the BSs have downloaded the pre-trained DNN models from cloud servers in advance [15].

The overall process of accomplishing the inference tasks in the edge computing system is composed of the following three phases.

- *Uplink Transmission:* The MDs upload the collected input data $\{d_k, k \in \mathcal{K}\}$ to the BSs.
- *Inference Computation:* The BSs feed data (e.g., d_k) into a specific pre-trained DNN model (e.g., ϕ_k) according to the task type and then obtain the inference results (e.g., $\phi_k(d_k)$).

- *Downlink Transmission:* The BSs deliver the inference results $\{\phi_k(d_k), k \in \mathcal{K}\}$ to the corresponding MDs.

By exploiting the broadcast nature of wireless channels, each MD's data can be successfully received by multiple BSs in the uplink, which enables the computation replication and creates multiple copies of the inference results at different BSs [27]. In the downlink, the BSs performing the same inference task cooperatively transmit the inference results to the corresponding MD [30]. To enable transmission cooperation among the BSs, it is assumed that the global channel state information (CSI) is available at the BSs. Let $\mathcal{A}_n \subseteq \mathcal{K}$ denote the set of MD indices whose inference tasks are selectively performed by BS n. For notational ease, we denote $\mathcal{A} = (\mathcal{A}_1, \ldots, \mathcal{A}_N)$ as the task selection strategy.

1) Uplink Transmission: Let $s_k^{\mathrm{UL}} \in \mathbb{C}$ denote the representative information symbol of input data d_k, and $p_k^{\mathrm{UL}} \in \mathbb{R}$ denote the transmit power of MD k. Without loss of generality, $\{s_k^{\mathrm{UL}}, k \in \mathcal{K}\}$ are assumed to have zero mean and unit power. The signal received at BS n can be expressed as

$$\boldsymbol{y}_n^{\mathrm{UL}} = \sum_{k \in \mathcal{K}} \boldsymbol{g}_{nk}^{\mathrm{UL}} \sqrt{p_k^{\mathrm{UL}}} s_k^{\mathrm{UL}} + \boldsymbol{z}_n^{\mathrm{UL}}, \tag{1}$$

where $\boldsymbol{g}_{nk}^{\mathrm{UL}} \in \mathbb{C}^{L_n \times 1}$ is the equivalent baseband channel response from MD k to BS n and $\boldsymbol{z}_n^{\mathrm{UL}} \sim \mathcal{CN}\left(\boldsymbol{0}, \sigma_n^2 \boldsymbol{I}_{L_n}\right)$ is the additive white Gaussian noise (AWGN) at BS n with σ_n^2 being the noise power. With the deployment of an RIS, the equivalent baseband channel from MD k to BS n consists of both the direct link and the reflected link, where the reflected link is a concatenation of the MD-RIS link, the phase shifts at the RIS, and the RIS-BS link [19], [23]-[26]. Therefore, $\boldsymbol{g}_{nk}^{\mathrm{UL}}$ can be modeled as

$$\boldsymbol{g}_{nk}^{\mathrm{UL}} = \underbrace{\boldsymbol{h}_{\mathrm{d},nk}^{\mathrm{UL}}}_{\text{direct link}} + \underbrace{\left(\boldsymbol{G}_n^{\mathrm{UL}}\right)^{\mathsf{H}} \left(\boldsymbol{\Theta}^{\mathrm{UL}}\right)^{\mathsf{H}} \boldsymbol{h}_{\mathrm{r},k}^{\mathrm{UL}}}_{\text{reflected link}}, \tag{2}$$

where $\boldsymbol{h}_{\mathrm{d},nk}^{\mathrm{UL}} \in \mathbb{C}^{L_n \times 1}$, $\boldsymbol{h}_{\mathrm{r},k}^{\mathrm{UL}} \in \mathbb{C}^{M \times 1}$, and $\boldsymbol{G}_n^{\mathrm{UL}} \in \mathbb{C}^{M \times L_n}$ denote the channel responses from MD k to BS n, from MD k to the RIS, and from the RIS to BS n, respectively. In addition, $\boldsymbol{\Theta}^{\mathrm{UL}} = \beta \mathrm{diag}\left(\theta_1^{\mathrm{UL}}, \ldots, \theta_M^{\mathrm{UL}}\right) \in \mathbb{C}^{M \times M}$ denotes the diagonal phase-shift matrix for uplink transmission, where $\beta \in [0, 1]$ is the amplitude reflection coefficient and $\theta_m^{\mathrm{UL}} = e^{j\varphi_m^{\mathrm{UL}}}$ with $\varphi_m^{\mathrm{UL}} \in [0, 2\pi)$ being the uplink phase shift of the m-th reflecting element of the RIS. The reflected link only accounts for one-time reflection, because the power of signals reflected by two or more times is negligible due to the high path loss [19], [23]-[26].

We consider the linear beamforming strategy, and denote the receive beamforming vector of BS n to decode s_k^{UL} as $\boldsymbol{v}_{nk}^{\mathrm{UL}} \in \mathbb{C}^{L_n \times 1}$. BS n only decodes MD k's transmitted symbol s_k^{UL} if $k \in \mathcal{A}_n$. The estimated symbol at BS n for MD $k \in \mathcal{A}_n$, denoted by $\hat{s}_{nk}^{\mathrm{UL}} \in \mathbb{C}$, is given by

$$\hat{s}_{nk}^{\mathrm{UL}} = \left(\boldsymbol{v}_{nk}^{\mathrm{UL}}\right)^{\mathsf{H}} \boldsymbol{y}_n^{\mathrm{UL}} = \left(\boldsymbol{v}_{nk}^{\mathrm{UL}}\right)^{\mathsf{H}} \boldsymbol{g}_{nk}^{\mathrm{UL}} \sqrt{p_k^{\mathrm{UL}}} s_k^{\mathrm{UL}}$$
$$+ \left(\boldsymbol{v}_{nk}^{\mathrm{UL}}\right)^{\mathsf{H}} \sum_{l \neq k} \boldsymbol{g}_{nl}^{\mathrm{UL}} \sqrt{p_l^{\mathrm{UL}}} s_l^{\mathrm{UL}} + \left(\boldsymbol{v}_{nk}^{\mathrm{UL}}\right)^{\mathsf{H}} \boldsymbol{z}_n^{\mathrm{UL}}. \tag{3}$$

Therefore, the uplink signal-to-interference-plus-noise ratio (SINR) observed at BS n for MD $k \in \mathcal{A}_n$ is

$$\text{SINR}_{nk}^{\text{UL}} = \frac{p_k^{\text{UL}} \left| \left(\boldsymbol{v}_{nk}^{\text{UL}} \right)^{\mathsf{H}} \boldsymbol{g}_{nk}^{\text{UL}} \right|^2}{\sum_{l \neq k} p_l^{\text{UL}} \left| \left(\boldsymbol{v}_{nk}^{\text{UL}} \right)^{\mathsf{H}} \boldsymbol{g}_{nl}^{\text{UL}} \right|^2 + \sigma_n^2 \left\| \boldsymbol{v}_{nk}^{\text{UL}} \right\|_2^2}. \tag{4}$$

2) Downlink Transmission: After performing the inference tasks, the BSs cooperatively transmit the inference results $\{\phi_k(d_k), k \in \mathcal{K}\}$ to the corresponding MDs through downlink wireless channels. Let $s_k^{\text{DL}} \in \mathbb{C}$ denote the representative symbol of $\phi_k(d_k)$ intended for MD k and $\boldsymbol{v}_{nk}^{\text{DL}}$ denote the downlink beamforming vector from BS n to MD k. Without loss of generality, $\{s_k^{\text{DL}}, \ k \in \mathcal{K}\}$ are assumed to have zero mean and unit power. The signal transmitted by BS n, denoted as $\boldsymbol{x}_n^{\text{DL}} \in \mathbb{C}^{L_n \times 1}$, is a summation of beamformed symbols for MD $k \in \mathcal{A}_n$, i.e.,

$$\boldsymbol{x}_n^{\text{DL}} = \sum_{k \in \mathcal{A}_n} \boldsymbol{v}_{nk}^{\text{DL}} s_k^{\text{DL}}, \ \forall n \in \mathcal{N}.$$

The signal received by MD k can be expressed as

$$
\begin{aligned}
y_k^{\text{DL}} &= \sum_{n \in \mathcal{N}} \left(\boldsymbol{g}_{nk}^{\text{DL}} \right)^{\mathsf{H}} \boldsymbol{x}_n^{\text{DL}} + z_k^{\text{DL}} \\
&= \sum_{n \in \mathcal{N}} \left(\boldsymbol{g}_{nk}^{\text{DL}} \right)^{\mathsf{H}} \left(\mathbf{1}_{\{k \in \mathcal{A}_n\}} \boldsymbol{v}_{nk}^{\text{DL}} s_k^{\text{DL}} + \sum_{\substack{l \neq k, \\ l \in \mathcal{A}_n}} \boldsymbol{v}_{nl}^{\text{DL}} s_l^{\text{DL}} \right) + z_k^{\text{DL}} \\
&= \sum_{n \in \mathcal{N}} \mathbf{1}_{\{k \in \mathcal{A}_n\}} \left(\boldsymbol{g}_{nk}^{\text{DL}} \right)^{\mathsf{H}} \boldsymbol{v}_{nk}^{\text{DL}} s_k^{\text{DL}} \\
&\quad + \sum_{l \neq k} \sum_{n \in \mathcal{N}} \mathbf{1}_{\{l \in \mathcal{A}_n\}} \left(\boldsymbol{g}_{nk}^{\text{DL}} \right)^{\mathsf{H}} \boldsymbol{v}_{nl}^{\text{DL}} s_l^{\text{DL}} + z_k^{\text{DL}}, \tag{5}
\end{aligned}
$$

where $z_k^{\text{DL}} \in \mathbb{C}$ is the AWGN at MD k with zero mean and power σ_k^2, and $\left(\boldsymbol{g}_{nk}^{\text{DL}} \right)^{\mathsf{H}} \in \mathbb{C}^{1 \times L_n}$ is the equivalent downlink channel response from BS n to MD k. Similar to the uplink counterpart, $\left(\boldsymbol{g}_{nk}^{\text{DL}} \right)^{\mathsf{H}}$ can be modeled as

$$\left(\boldsymbol{g}_{nk}^{\text{DL}} \right)^{\mathsf{H}} = \underbrace{\left(\boldsymbol{h}_{\text{d},nk}^{\text{DL}} \right)^{\mathsf{H}}}_{\text{direct link}} + \underbrace{\left(\boldsymbol{h}_{\text{r},k}^{\text{DL}} \right)^{\mathsf{H}} \boldsymbol{\Theta}^{\text{DL}} \boldsymbol{G}_n^{\text{DL}}}_{\text{reflected link}}, \tag{6}$$

where $\left(\boldsymbol{h}_{\text{d},nk}^{\text{DL}} \right)^{\mathsf{H}} \in \mathbb{C}^{1 \times L_n}$, $\left(\boldsymbol{h}_{\text{r},k}^{\text{DL}} \right)^{\mathsf{H}} \in \mathbb{C}^{1 \times M}$, and $\boldsymbol{G}_n^{\text{DL}} \in \mathbb{C}^{M \times L_n}$ denote the channel responses from BS n to MD k, from the RIS to MD k, and from BS n to the RIS, respectively, and $\boldsymbol{\Theta}^{\text{DL}} = \beta \text{diag} \left(\theta_1^{\text{DL}}, \ldots, \theta_M^{\text{DL}} \right) \in \mathbb{C}^{M \times M}$ is the downlink phase-shift matrix with diagonal entries $\theta_m^{\text{DL}} = e^{j \varphi_m^{\text{DL}}}$ and $\varphi_m^{\text{DL}} \in [0, 2\pi)$.

Based on (5), the SINR observed by MD $k \in \mathcal{K}$ in the downlink is given by

$$\text{SINR}_k^{\text{DL}}(\mathcal{A}) = \frac{\left| \sum_{n \in \mathcal{N}} \mathbf{1}_{\{k \in \mathcal{A}_n\}} \left(\boldsymbol{g}_{nk}^{\text{DL}} \right)^{\mathsf{H}} \boldsymbol{v}_{nk}^{\text{DL}} \right|^2}{\sum_{l \neq k} \left| \sum_{n \in \mathcal{N}} \mathbf{1}_{\{l \in \mathcal{A}_n\}} \left(\boldsymbol{g}_{nk}^{\text{DL}} \right)^{\mathsf{H}} \boldsymbol{v}_{nl}^{\text{DL}} \right|^2 + \sigma_k^2}. \tag{7}$$

B. Power Consumption Model

As running DNN models often incurs high energy consumption due to their high computational complexity [31], [32],

and energy-efficiency is one of the key performance indicators for green communications [33], in this subsection, we present the power consumption model in the proposed edge inference system, taking into consideration both the computation power for inference and the communication power for uplink and downlink transmissions.

1) Computation Power Consumption: We denote the power consumption of performing MD k's inference task at BS n as P_{nk}^{c}. As a result, the total computation power consumption at all BSs is given by

$$P_{\text{comp}}(\mathcal{A}) = \sum_{n \in \mathcal{N}} \sum_{k \in \mathcal{A}_n} P_{nk}^{\text{c}}. \tag{8}$$

It is worth noting that the majority of the computation power is consumed for running DNN models, and it can be estimated by using the energy estimation methodology proposed in [31]. This methodology provides a layer-wise energy breakdown for arbitrary neural networks. In particular, the DNN configurations (e.g., number of filters, number of input feature maps) are taken as inputs and the normalized layer-wise consumptions energy of the neural network (i.e., the energy consumption per multiply-and-accumulation (MAC) operation) are generated as outputs [34]. The computation time can be calculated via dividing the number of MAC operations by the average throughput of a CPU chip. Therefore, the power consumption for performing an inference task equals to the total energy consumption divided by the corresponding computation time.

For example, the energy consumption of running a widely used DNN model AlexNet to process one image on a well-designed energy-efficient Eyeriss chip can be approximated by that of performing 4×10^9 MAC operations, and the typical value of the power consumption for processing an image using AlexNet on a Eyeriss Chip at core supply voltage $1.2\,\text{V}$ is $0.45\,\text{W}$ [35]. As the typical value of computation power P_{nk}^{c} (e.g., $0.45\,\text{W}$) is comparable to the BSs' transmit power (e.g., $1\,\text{W}$ [36]), it is necessary to take into account both the computation and transmit power to facilitate the energy-efficient design.

2) Communication Power Consumption: The communication power consumption consists of the power consumed by the MDs in the uplink transmission and by the BSs in the downlink transmission. According to (2)-(7), the total uplink transmit power consumption is $\sum_{k \in \mathcal{K}} p_k^{\text{UL}}$, while the downlink transmit power consumption of BS n is given by

$$\mathbf{E}\left[\sum_{k \in \mathcal{A}_n} \left\| \boldsymbol{v}_{nk}^{\text{DL}} s_k^{\text{DL}} \right\|_2^2 \right] = \sum_{k \in \mathcal{A}_n} \left\| \boldsymbol{v}_{nk}^{\text{DL}} \right\|_2^2,$$

where $\mathbf{E}[\cdot]$ denotes the expectation. Therefore, the total communication power consumption for both uplink and downlink transmissions is given by

$$P_{\text{comm}}(\mathcal{A}, \{p_k^{\text{UL}}\}, \{\boldsymbol{v}_{nk}^{\text{DL}}\}) = \sum_{k \in \mathcal{K}} p_k^{\text{UL}} + \sum_{n \in \mathcal{N}} \sum_{k \in \mathcal{A}_n} \frac{1}{\eta_n} \left\| \boldsymbol{v}_{nk}^{\text{DL}} \right\|_2^2,$$

where η_n is the drain efficiency coefficient of the radio frequency power amplifier of BS n.

The overall network power consumption, consisting of both the computation power and communication power, can be expressed as

$$P_{\text{total}}(\mathcal{A}, \{p_k^{\text{UL}}\}, \{\boldsymbol{v}_{nk}^{\text{DL}}\}) = P_{\text{comm}}(\mathcal{A}, \{p_k^{\text{UL}}\}, \{\boldsymbol{v}_{nk}^{\text{DL}}\}) + P_{\text{comp}}(\mathcal{A})$$

$$= \sum_{k \in \mathcal{K}} p_k^{\text{UL}} + \sum_{n \in \mathcal{N}} \sum_{k \in \mathcal{A}_n} \frac{1}{\eta_n} \left\| \boldsymbol{v}_{nk}^{\text{DL}} \right\|_2^2 + \sum_{n \in \mathcal{N}} \sum_{k \in \mathcal{A}_n} P_{nk}^{\text{c}}. \quad (9)$$

C. Problem Formulation and Analysis

In the proposed edge inference system, there exists a fundamental tradeoff between communication and computation power consumption. Specifically, with computation replication, more BSs performing the same task can reduce the downlink transmission power consumption by exploiting a higher cooperative beamforming gain, at the cost of increasing the computation power consumption. Therefore, we propose to achieve green edge inference by minimizing the overall network power consumption via striking a balance between the communication and computation power consumption.

Let $\{\gamma_k^{\text{UL}}, k \in \mathcal{K}\}$ and $\{\gamma_k^{\text{DL}}, k \in \mathcal{K}\}$ denote the SINR thresholds required to successfully receive the input data and inference results in the uplink and downlink, respectively. The overall network power consumption minimization problem is formulated as

$$\mathscr{P}_{\text{original}} : \min_{\substack{\mathcal{A}, \{\boldsymbol{v}_{nk}^{\text{DL}}\}, \boldsymbol{\Theta}^{\text{DL}}, \\ \{\boldsymbol{v}_{nk}^{\text{UL}}\}, \{p_k^{\text{UL}}\}, \boldsymbol{\Theta}^{\text{UL}}}} P_{\text{total}}(\mathcal{A}, \{p_k^{\text{UL}}\}, \{\boldsymbol{v}_{nk}^{\text{DL}}\})$$

$$\text{subject to } \text{SINR}_k^{\text{DL}}(\mathcal{A}) \geq \gamma_k^{\text{DL}}, \quad \forall k \in \mathcal{K}, \quad (10a)$$

$$\text{SINR}_{nk}^{\text{UL}} \geq \gamma_k^{\text{UL}}, \forall k \in \mathcal{A}_n, n \in \mathcal{N}, (10b)$$

$$\sum_{k \in \mathcal{A}_n} \left\| \boldsymbol{v}_{nk}^{\text{DL}} \right\|_2^2 \leq P_{n,\max}^{\text{DL}}, \quad \forall n \in \mathcal{N}, (10c)$$

$$p_k^{\text{UL}} \leq P_{k,\max}^{\text{UL}}, \quad \forall k \in \mathcal{K}, \quad (10d)$$

$$|\theta_m^{\text{DL}}| = 1, \quad \forall m \in \mathcal{M}, \quad (10e)$$

$$|\theta_m^{\text{UL}}| = 1, \quad \forall m \in \mathcal{M}, \quad (10f)$$

where $P_{k,\max}^{\text{UL}}$ denotes the maximum transmit power of MD k in the uplink and $P_{n,\max}^{\text{DL}}$ denotes the maximum transmit power of BS n in the downlink.

In order to solve problem $\mathscr{P}_{\text{original}}$, we are confronted with several main challenges. Problem $\mathscr{P}_{\text{original}}$ is a mixed combinatorial optimization problem with nonconvex constraints, which is highly intractable. Besides the troublesome combinatorial variable $\mathcal{A}$, the coupled continuous variables phases shifts and beamforming vectors in constraints (10a)-(10b) pose a unique challenge. Moreover, the unit-modulus constraints (10e)-(10f) imposed by the phase-shift of each RIS element are nonconvex. In the following, we shall propose a group sparse reformulation for the overall network power minimization problem, so as to get rid of the combinatorial variable $\mathcal{A}$ in $\mathscr{P}_{\text{original}}$ and thereby facilitating efficient algorithm design.

D. Group Sparse Reformulation

By exploiting the intrinsic connection between the task selection (i.e., $\mathcal{A}$) and the group sparsity structure of beamforming vector $\boldsymbol{v}_{nk} = \left[\left(\boldsymbol{v}_{nk}^{\text{UL}}\right)^{\mathsf{T}}, \left(\boldsymbol{v}_{nk}^{\text{DL}}\right)^{\mathsf{T}} \right]^{\mathsf{T}}$, the combinatorial variable

$\mathcal{A}$ can be eliminated. Specifically, if $k \notin \mathcal{A}_n$, BS n does not decode MD k's data in the uplink (i.e., $\boldsymbol{v}_{nk}^{\text{UL}} = \boldsymbol{0}$) and subsequently cannot transmit inference results to MD k in the downlink (i.e., $\boldsymbol{v}_{nk}^{\text{DL}} = \boldsymbol{0}$). In other words, all coefficients in the beamforming group $\boldsymbol{v}_{nk}$ are zero simultaneously if $k \notin \mathcal{A}_n$. As multiple tasks may not be performed by a certain BS, the aggregated beamforming vector $\boldsymbol{v} \in \mathbb{C}^{K \sum_{n=1}^N L_n}$ defined as $\boldsymbol{v} = \left[\boldsymbol{v}_{11}^{\mathsf{T}}, \ldots, \boldsymbol{v}_{1K}^{\mathsf{T}}, \ldots, \boldsymbol{v}_{N1}^{\mathsf{T}}, \ldots, \boldsymbol{v}_{NK}^{\mathsf{T}}\right]^{\mathsf{T}}$ is expected to have the group sparsity structure with only a few non-zero blocks.

The above discussions indicate that the task selection strategy $\mathcal{A}$ can be determined by the group sparsity pattern of the beamforming groups, i.e., $\mathcal{A}_n = \{k|\boldsymbol{v}_{nk} \neq \boldsymbol{0}, \ k \in \mathcal{K}\}, \ \forall n \in \mathcal{N}$. Therefore, the overall network power consumption (9) can be equivalently rewritten as

$$P_{\text{total}}(\{p_k^{\text{UL}}\}, \{\boldsymbol{v}_{nk}^{\text{DL}}\}) = \sum_{k=1}^K p_k^{\text{UL}} + \sum_{n=1}^N \sum_{k=1}^K \frac{1}{\eta_n} \left\| \boldsymbol{v}_{nk}^{\text{DL}} \right\|_2^2$$

$$+ \sum_{n=1}^N \sum_{k=1}^K \mathbf{1}_{\{\boldsymbol{v}_{nk}=\boldsymbol{0}\}} P_{nk}^{\text{c}}. \quad (11)$$

In addition, the $\text{SINR}_{nk}^{\text{UL}}$ expression in (4) can be rewritten as

$$\text{SINR}_{nk}^{\text{UL}} = \frac{p_k^{\text{UL}} \left| \left(\boldsymbol{v}_{nk}^{\text{UL}}\right)^{\mathsf{H}} \boldsymbol{g}_{nk}^{\text{UL}} \right|^2}{\sum_{l \neq k} p_l^{\text{UL}} \left| \left(\boldsymbol{v}_{nk}^{\text{UL}}\right)^{\mathsf{H}} \boldsymbol{g}_{nl}^{\text{UL}} \right|^2 + \sigma_n^2 \left\| \boldsymbol{v}_{nk}^{\text{UL}} \right\|_2^2}, \ \forall n, \forall k \in \mathcal{K},$$

where $\boldsymbol{v}_{nk}^{\text{UL}} = \boldsymbol{0}$ if $k \notin \mathcal{A}_n$, and $\text{SINR}_k^{\text{DL}}$ expression in (7) can be simplified as

$$\text{SINR}_k^{\text{DL}} = \frac{\left| \sum_{n=1}^N \left(\boldsymbol{g}_{nk}^{\text{DL}}\right)^{\mathsf{H}} \boldsymbol{v}_{nk}^{\text{DL}} \right|^2}{\sum_{l \neq k} \left| \sum_{n=1}^N \left(\boldsymbol{g}_{nk}^{\text{DL}}\right)^{\mathsf{H}} \boldsymbol{v}_{nl}^{\text{DL}} \right|^2 + \sigma_k^2}, \ \forall k, \quad (12)$$

where $\boldsymbol{v}_{nk}^{\text{DL}} = \boldsymbol{0}$ if $k \notin \mathcal{A}_n$. Problem $\mathscr{P}_{\text{original}}$ is then equivalent to the following group sparse beamforming problem

$$\mathscr{P} : \min_{\substack{\{\boldsymbol{v}_{nk}^{\text{DL}}\}, \boldsymbol{\Theta}^{\text{DL}}, \\ \{\boldsymbol{v}_{nk}^{\text{UL}}\}, \{p_k^{\text{UL}}\}, \boldsymbol{\Theta}^{\text{UL}}}} P_{\text{total}}(\{p_k^{\text{UL}}\}, \{\boldsymbol{v}_{nk}^{\text{DL}}\})$$

$$\text{subject to } \text{SINR}_k^{\text{DL}} \geq \gamma_k^{\text{DL}}, \quad \forall k \in \mathcal{K}, \quad (13a)$$

$$\text{SINR}_{nk}^{\text{UL}} \geq \gamma_k^{\text{UL}}, \quad \forall n \in \mathcal{N}, \ k \in \mathcal{K}, (13b)$$

$$\sum_{k=1}^K \left\| \boldsymbol{v}_{nk}^{\text{DL}} \right\|_2^2 \leq P_{n,\max}^{\text{DL}}, \ \forall n \in \mathcal{N}, \quad (13c)$$

$$p_k^{\text{UL}} \leq P_{k,\max}^{\text{UL}}, \quad \forall k \in \mathcal{K}, \quad (13d)$$

$$|\theta_m^{\text{DL}}| = 1, \quad \forall m \in \mathcal{M}, \quad (13e)$$

$$|\theta_m^{\text{UL}}| = 1, \quad \forall m \in \mathcal{M}, \quad (13f)$$

where we aim to induce the group sparsity of beamforming vector $\boldsymbol{v}$. The equivalence means that if $\left(\{\boldsymbol{v}_{nk}^{\text{UL}}\}, \{p_k^{\text{UL}}\}, \{\boldsymbol{v}_{nk}^{\text{DL}}\}, \boldsymbol{\Theta}^{\text{UL}}, \boldsymbol{\Theta}^{\text{DL}}\right)$ is a solution to problem $\mathscr{P}$, then $\left(\mathcal{A}, \{\boldsymbol{v}_{nk}^{\text{UL}}\}, \{p_k^{\text{UL}}\}, \{\boldsymbol{v}_{nk}^{\text{DL}}\}, \boldsymbol{\Theta}^{\text{UL}}, \boldsymbol{\Theta}^{\text{DL}}\right)$ with $\mathcal{A}_n = \{k|\boldsymbol{v}_{nk} \neq \boldsymbol{0}, \ k \in \mathcal{K}\}, \ \forall n \in \mathcal{N}$ is also a solution to problem $\mathscr{P}_{\text{original}}$ achieving the same objective value, and vice versa.

Solving problem $\mathscr{P}$ calls for a joint design of beamforming vectors, transmit power, and phase shifts. As the optimization variables are coupled with each other in constraints (13a) and

(13b), in the next section, we shall propose a BSO approach to effectively decouple the optimization variables.

III. BLOCK-STRUCTURED OPTIMIZATION APPROACH

In this section, we propose a BSO approach to decouple the optimization variables. The main idea of the BSO approach is to partition the variables into several blocks, and alternatively optimize one of the blocks in each iteration while keeping the others fixed [37]. Specifically, we partition the five optimization variables into three blocks, denoted as $\mathcal{B}_1 = \left(\{\boldsymbol{v}_{nk}^{\mathrm{DL}}\}, \{\boldsymbol{v}_{nk}^{\mathrm{UL}}\}, \{p_k^{\mathrm{UL}}\}\right)$, $\mathcal{B}_2 = \boldsymbol{\Theta}^{\mathrm{DL}}$, and $\mathcal{B}_3 = \boldsymbol{\Theta}^{\mathrm{UL}}$. The main motivation for such a partition is that for given $\boldsymbol{\Theta}^{\mathrm{UL}}$ and $\boldsymbol{\Theta}^{\mathrm{DL}}$, problem $\mathscr{P}$ is reduced to a well-studied joint uplink and downlink power minimization problem.

A. Optimizing Variables $\{\boldsymbol{v}_{nk}^{UL}\}$, $\{p_k^{UL}\}$, and $\{\boldsymbol{v}_{nk}^{DL}\}$

When $\mathcal{B}_2$ and $\mathcal{B}_3$ are fixed, problem $\mathscr{P}$ is reduced to the following problem

$$\mathscr{P}_1 : \quad \underset{\{\boldsymbol{v}_{nk}^{\mathrm{DL}}\}, \{\boldsymbol{v}_{nk}^{\mathrm{UL}}\}, \{p_k^{\mathrm{UL}}\}}{\mathrm{minimize}} \quad P_{\mathrm{total}}(\{p_k^{\mathrm{UL}}\}, \{\boldsymbol{v}_{nk}^{\mathrm{DL}}\})$$
$$\mathrm{subject~to} \quad (13\mathrm{a}) - (13\mathrm{d}).$$

It is observed that $\boldsymbol{v}_{nk}^{\mathrm{UL}}$ and $\boldsymbol{v}_{nk}^{\mathrm{DL}}$ are only coupled in the objective function. For the sake of analysis convenience and efficient algorithm design, we temporarily dismiss the indicator function in the objective function and split problem $\mathscr{P}_1$ into two parts, i.e., the downlink part $\mathscr{P}_{1\text{-}1}$ and the uplink part $\mathscr{P}_{1\text{-}2}$.

Specifically, the power minimization problem in the downlink part is

$$\mathscr{P}_{1\text{-}1} : \quad \underset{\{\boldsymbol{v}_{nk}^{\mathrm{DL}}\}}{\mathrm{minimize}} \quad \sum_{n=1}^{N} \sum_{k=1}^{K} \frac{1}{\eta_n} \left\| \boldsymbol{v}_{nk}^{\mathrm{DL}} \right\|_2^2$$
$$\mathrm{subject~to} \quad (13\mathrm{a}), (13\mathrm{c}),$$

which is a celebrated problem formulation in unicast multiple-input single-output (MISO) systems. Due to the fact that an arbitrary phase rotation of transmit beamforming vectors does not affect the SINR constraints (13a) [38], we can replace (13a) with the following second-order cone (SOC) constraint

$$\sqrt{\sum_{l \neq k} \left| \left(\boldsymbol{g}_k^{\mathrm{DL}}\right)^{\mathsf{H}} \boldsymbol{v}_l^{\mathrm{DL}} \right|^2 + \sigma_k^2} \leq \frac{1}{\sqrt{\gamma_k^{\mathrm{DL}}}} \Re\left(\left(\boldsymbol{g}_k^{\mathrm{DL}}\right)^{\mathsf{H}} \boldsymbol{v}_k^{\mathrm{DL}} \right), \quad (14)$$

where $\boldsymbol{g}_k^{\mathrm{DL}} = \left[\left(\boldsymbol{g}_{1k}^{\mathrm{DL}}\right)^{\mathsf{T}}, \ldots, \left(\boldsymbol{g}_{Nk}^{\mathrm{DL}}\right)^{\mathsf{T}} \right]^{\mathsf{T}}$ and $\boldsymbol{v}_k^{\mathrm{DL}} = \left[\left(\boldsymbol{v}_{1k}^{\mathrm{DL}}\right)^{\mathsf{T}}, \ldots, \left(\boldsymbol{v}_{Nk}^{\mathrm{DL}}\right)^{\mathsf{T}} \right]^{\mathsf{T}}$ denote the aggregated channel response vector and transmit beamforming vector with respect to MD k, respectively. Therefore, problem $\mathscr{P}_{1\text{-}1}$ is recast as a convex second-order cone programming (SOCP), which can be effectively solved by interior-point methods using modern software like CVX [39].

On the other hand, the power minimization problem in the uplink is given by

$$\mathscr{P}_{1\text{-}2} : \quad \underset{\{\boldsymbol{v}_{nk}^{\mathrm{UL}}\}, \{p_k^{\mathrm{UL}}\}}{\mathrm{minimize}} \quad \sum_{k=1}^{K} p_k^{\mathrm{UL}}$$
$$\mathrm{subject~to} \quad (13\mathrm{b}), (13\mathrm{d}).$$

Although the SINR constraints (13b) are similar to those in the downlink counterpart, we cannot convexify them in a similar way. The main reason is that the phase rotation of the receive beamforming vector $\boldsymbol{v}_{nk}^{\mathrm{UL}}$ cannot guarantee both numerator and denominator of the uplink SINR expression defined in (4) to be real numbers. Moreover, another issue in $\mathscr{P}_{1\text{-}2}$ is that directly optimizing this problem makes $\boldsymbol{v}_{nk}^{\mathrm{UL}}$ to be nearly zero, because an arbitrary scaling of $\boldsymbol{v}_{nk}^{\mathrm{UL}}$ does not affect the uplink SINR constraints (13b) [40]. Specifically, if $\left(\tilde{\boldsymbol{v}}_{nk}^{\mathrm{UL}}, \tilde{p}_k^{\mathrm{UL}}\right)$ denotes the optimal solution to problem $\mathscr{P}_{1\text{-}2}$, then we have

$$\tilde{\boldsymbol{v}}_{nk}^{\mathrm{UL}} \approx \boldsymbol{0}, \ \forall n \in \mathcal{N}, \ k \in \mathcal{K}. \quad (15)$$

Although (15) does not violate the group sparsity structure of $\boldsymbol{v}_{nk}$, it indicates that the receive beamforming vectors do not contribute to the task selection. Based on the uplink-downlink duality, in the following, we shall propose a virtual downlink formulation to overcome the scaling issue.

To facilitate effective algorithm design, we relax problem $\mathscr{P}_{1\text{-}2}$ to the following problem

$$\underset{\{\boldsymbol{v}_{nk}^{\mathrm{UL}}\}, \{p_{nk}\}}{\mathrm{minimize}} \quad \frac{1}{N} \sum_{n=1}^{N} \sum_{k=1}^{K} p_{nk}$$
$$\mathrm{subject~to} \quad p_{nk} \leq P_{k,\max}^{\mathrm{UL}}, \ \forall n, \forall k, \quad (16\mathrm{a})$$

$$\frac{p_{nk} \left| \left(\boldsymbol{v}_{nk}^{\mathrm{UL}}\right)^{\mathsf{H}} \boldsymbol{g}_{nk}^{\mathrm{UL}} \right|^2}{\sum_{l \neq k} p_{nl} \left| \left(\boldsymbol{v}_{nk}^{\mathrm{UL}}\right)^{\mathsf{H}} \boldsymbol{g}_{nl}^{\mathrm{UL}} \right|^2 + \sigma_n^2 \left\| \boldsymbol{v}_{nk}^{\mathrm{UL}} \right\|_2^2} \geq \gamma_k^{\mathrm{UL}}, \forall n, \forall k. \quad (16\mathrm{b})$$

We can easily verify that problem (16) is indeed a relaxation to problem $\mathscr{P}_{1\text{-}2}$, because given any solution $\left(\{\boldsymbol{v}_{nk}^{\mathrm{UL}}\}, \{p_k^{\mathrm{UL}}\}\right)$ feasible to problem $\mathscr{P}_{1\text{-}2}$, $\left(\{\boldsymbol{v}_{nk}^{\mathrm{UL}}\}, \{p_{nk}\}\right)$ is also feasible to problem (16) when $p_{nk} = p_k^{\mathrm{UL}}, \forall n \in \mathcal{N}$, and the objective value of problem (16) is no greater than that of $\mathscr{P}_{1\text{-}2}$. The motivation for this relaxation is that problem (16) can be solved in the virtual downlink formulation so as to overcome the scaling issue.

We first consider an ideal scenario that the MDs have unlimited power budgets (i.e., $P_{k,\max}^{\mathrm{UL}} = +\infty, \forall k \in \mathcal{K}$). Problem (16) is then equivalent to the following virtual downlink power minimization problem

$$\underset{\{\boldsymbol{v}_{nk}^{\mathrm{VDL}}\}}{\mathrm{minimize}} \quad \frac{1}{N} \sum_{n=1}^{N} \sum_{k=1}^{K} \left\| \boldsymbol{v}_{nk}^{\mathrm{VDL}} \right\|_2^2 \quad (17\mathrm{a})$$
$$\mathrm{subject~to} \quad \mathrm{SINR}_{nk}^{\mathrm{VDL}} \geq \gamma_k^{\mathrm{UL}}, \ \forall n, \forall k, \quad (17\mathrm{b})$$

where $\boldsymbol{v}_{nk}^{\mathrm{VDL}} \in \mathbb{C}^{L_n \times 1}$ denotes the virtual downlink transmit beamforming vector from BS n to MD k, and $\mathrm{SINR}_{nk}^{\mathrm{VDL}}$ is the virtual downlink SINR observed by MD k defined as

$$\mathrm{SINR}_{nk}^{\mathrm{VDL}} = \frac{\left| \left(\boldsymbol{g}_{nk}^{\mathrm{UL}}\right)^{\mathsf{H}} \boldsymbol{v}_{nk}^{\mathrm{VDL}} \right|^2}{\sum_{l \neq k} \left| \left(\boldsymbol{g}_{nk}^{\mathrm{UL}}\right)^{\mathsf{H}} \boldsymbol{v}_{nl}^{\mathrm{VDL}} \right|^2 + \sigma_n^2}. \quad (18)$$

It is noticed that in (18), the scaling issue no longer exists for $\{\boldsymbol{v}_{nk}^{\mathrm{VDL}}, n \in \mathcal{N}, k \in \mathcal{K}\}$. The rigorous proof of the equivalence of the uplink power minimization problem (16) and the virtual downlink problem (17) can be derived by Lagrangian duality, as in [41, Theorem 1]. The optimal

solutions obtained by solving problem (17) have close connections to solutions to problem (16), i.e., $v_{nk}^{\text{VDL}} = v_{nk}^{\text{UL}}$ and $\sum_{n=1}^{N} \sum_{k=1}^{K} \left\| v_{nk}^{\text{VDL}} \right\|_2^2 = \sum_{n=1}^{N} \sum_{k=1}^{K} p_{nk}$. However, it is worth mentioning that the equivalence between the virtual downlink beamforming power and the uplink transmit power does not necessarily hold, i.e., $\left\| v_{nk}^{\text{VDL}} \right\|_2^2 \neq p_{nk}$. Therefore if $P_{k,\max}^{\text{UL}} < +\infty$, we cannot directly rewrite the transmit power constraints (16a) as $\left\| v_{nk}^{\text{VDL}} \right\|_2^2 \leq P_{k,\max}^{\text{UL}}, \forall n, \forall k$ out of intuition and add them to problem (17). Instead, we consider a sum-power constraint to relax the uplink transmit power constraints (16a), which is given by

$$\sum_{n=1}^{N} \sum_{k=1}^{K} \left\| v_{nk}^{\text{VDL}} \right\|_2^2 = \sum_{n=1}^{N} \sum_{k=1}^{K} p_{nk} \leq N \sum_{k=1}^{K} P_{k,\max}^{\text{UL}}. \quad (19)$$

By introducing this mild power control to problem (17), we need to solve the following problem

$$\underset{\{v_{nk}^{\text{VDL}}\}}{\text{minimize}} \quad \frac{1}{N} \sum_{n=1}^{N} \sum_{k=1}^{K} \left\| v_{nk}^{\text{VDL}} \right\|_2^2$$
$$\text{subject to} \quad (17\text{b}), (19). \quad (20)$$

Similar to (14), constraint (17b) can be replaced with the following SOC constraint

$$\sqrt{\sum_{l \neq k} \left| \left(g_{nk}^{\text{UL}}\right)^{\mathsf{H}} v_{nl}^{\text{VDL}} \right|^2 + \sigma_n^2} \leq \frac{1}{\sqrt{\gamma_k^{\text{VDL}}}} \Re \left(\left(g_{nk}^{\text{UL}}\right)^{\mathsf{H}} v_{nk}^{\text{VDL}} \right) \quad (21)$$

to make problem (20) a convex SOCP problem.

By exploiting the uplink-downlink duality and transforming the uplink model into a virtual downlink model, we address the challenge of the receive beamforming vectors scaling issue. As $\{v_{nk}^{\text{VDL}}\}$ have the same group sparsity pattern as $\{v_{nk}^{\text{UL}}\}$, combining the downlink and virtual downlink parts, we relax $\mathscr{P}_1$ to the following problem

$$\underset{\{v_{nk}^{\text{VDL}}\}, \{v_{nk}^{\text{DL}}\}}{\text{minimize}} \quad \frac{1}{N} \sum_{n=1}^{N} \sum_{k=1}^{K} \left\| v_{nk}^{\text{VDL}} \right\|_2^2 + \sum_{n=1}^{N} \sum_{k=1}^{K} \frac{1}{\eta_n} \left\| v_{nk}^{\text{DL}} \right\|_2^2$$
$$+ \sum_{n=1}^{N} \sum_{k=1}^{K} \mathbf{1}_{\{\bar{v}_{nk} = \mathbf{0}\}} P_{nk}^{\text{c}}$$
$$\text{subject to} \quad (13\text{c}), (14), (19), (21), \quad (22)$$

where $\bar{v}_{nk}$ in the objective function is defined as $\bar{v}_{nk} = \left[\left(v_{nk}^{\text{VDL}}\right)^{\mathsf{T}}, \left(v_{nk}^{\text{DL}}\right)^{\mathsf{T}} \right]^{\mathsf{T}}$. It is observed that all the constraints of problem (22) are convex.

Once we solve problem (22) and obtain the solutions $\left(\{v_{nk}^{\text{DL}}\}, \{v_{nk}^{\text{VDL}}\}\right)$, the receive beamforming vector $\{v_{nk}^{\text{UL}}\}$ in $\mathscr{P}_1$ can be obtained by setting $v_{nk}^{\text{UL}} = v_{nk}^{\text{VDL}}, \forall n \in \mathcal{N}, k \in \mathcal{K}$, and $\{p_k^{\text{UL}}\}$ can be obtained by solving problem $\mathscr{P}_{1\text{-}2}$ with $\{v_{nk}^{\text{UL}}\}$ fixed, which is reduced to a linear program.

B. Optimizing Variable Θ^{DL}

For given $\mathcal{B}_1$ and $\mathcal{B}_3$, we optimize Θ^{DL} to solve the resulting problem, which is termed as $\mathscr{P}_2$. Since Θ^{DL} does not appear in

the objective function of $\mathscr{P}$, problem $\mathscr{P}_2$ is in fact a downlink feasibility detection problem, which is given by

$$\mathscr{P}_2: \quad \text{find} \quad \Theta^{\text{DL}}$$
$$\text{subject to} \quad (13\text{a}), (13\text{e}).$$

According to the SINR^{DL} expression given in (12), we have

$$\left| \sum_{n=1}^{N} \left(g_{nk}^{\text{DL}}\right)^{\mathsf{H}} v_{nl}^{\text{DL}} \right|^2$$
$$\overset{(a)}{=} \left| \sum_{n=1}^{N} \left(\left(h_{\text{d},nk}^{\text{DL}}\right)^{\mathsf{H}} + \left(h_{\text{r},k}^{\text{DL}}\right)^{\mathsf{H}} \Theta^{\text{DL}} G_n^{\text{DL}} \right) v_{nl}^{\text{DL}} \right|^2$$
$$\overset{(b)}{=} \left| \left(h_{\text{d},k}^{\text{DL}}\right)^{\mathsf{H}} v_l^{\text{DL}} + \beta \left(a^{\text{DL}}\right)^{\mathsf{H}} \text{diag} \left(\left(h_{\text{r},k}^{\text{DL}}\right)^{\mathsf{H}} \right) \tilde{G}^{\text{DL}} v_l^{\text{DL}} \right|^2, (23)$$

where (a) follows by substituting (6), and (b) holds by defining

$$h_{\text{d},k}^{\text{DL}} = \left[\left(h_{\text{d},1k}^{\text{DL}}\right)^{\mathsf{T}}, \ldots, \left(h_{\text{d},Nk}^{\text{DL}}\right)^{\mathsf{T}} \right]^{\mathsf{T}}, a^{\text{DL}} = \left[\theta_1^{\text{DL}}, \ldots, \theta_M^{\text{DL}} \right]^{\mathsf{H}},$$
$$v_l^{\text{DL}} = \left[\left(v_{1l}^{\text{DL}}\right)^{\mathsf{T}}, \ldots, \left(v_{Nl}^{\text{DL}}\right)^{\mathsf{T}} \right]^{\mathsf{T}}, \tilde{G}^{\text{DL}} = \left[G_1^{\text{DL}}, \ldots, G_N^{\text{DL}} \right].$$

Note that in (23) the only term related to phase shifts is a^{DL}. Therefore for notational ease, we define

$$w_{kl}^{\text{DL}} = \beta \text{diag} \left(\left(h_{\text{r},k}^{\text{DL}}\right)^{\mathsf{H}} \right) \tilde{G}^{\text{DL}} v_l^{\text{DL}}, \quad b_{kl}^{\text{DL}} = \left(h_{\text{d},k}^{\text{DL}}\right)^{\mathsf{H}} v_l^{\text{DL}},$$

and the SINR^{DL} expression in (12) can be equivalently rewritten as

$$\text{SINR}_k^{\text{DL}} = \frac{\left| b_{kk}^{\text{DL}} + \left(a^{\text{DL}}\right)^{\mathsf{H}} w_{kk}^{\text{DL}} \right|^2}{\sum_{l \neq k} \left| b_{kl}^{\text{DL}} + \left(a^{\text{DL}}\right)^{\mathsf{H}} w_{kl}^{\text{DL}} \right|^2 + \sigma_k^2}, \quad (24)$$

leading to the following inhomogeneous QCQP problem

$$\text{find} \quad a^{\text{DL}}$$
$$\text{subject to} \quad \left| a_m^{\text{DL}} \right|^2 = 1, \forall m, \quad (25\text{a})$$
$$\frac{\left| b_{kk}^{\text{DL}} + \left(a^{\text{DL}}\right)^{\mathsf{H}} w_{kk}^{\text{DL}} \right|^2}{\sum_{l \neq k} \left| b_{kl}^{\text{DL}} + \left(a^{\text{DL}}\right)^{\mathsf{H}} w_{kl}^{\text{DL}} \right|^2 + \sigma_k^2} \geq \gamma_k, \forall k. (25\text{b})$$

By introducing an auxiliary scalar t, and defining

$$R_{kl}^{\text{DL}} = \begin{bmatrix} w_{kl}^{\text{DL}} \left(w_{kl}^{\text{DL}}\right)^{\mathsf{H}} & w_{kl}^{\text{DL}} \left(b_{kl}^{\text{DL}}\right)^{\mathsf{H}} \\ \left(w_{kl}^{\text{DL}}\right)^{\mathsf{H}} b_{kl}^{\text{DL}} & 0 \end{bmatrix}, \bar{a}^{\text{DL}} = \begin{bmatrix} a^{\text{DL}} \\ t^{\text{DL}} \end{bmatrix},$$

problem (25) can be transformed into the following homogeneous QCQP problem [19]

$$\text{find} \quad \bar{a}^{\text{DL}}$$
$$\text{subject to} \quad \left| \bar{a}_m^{\text{DL}} \right|^2 = 1, \quad \text{for } m = 1, \ldots, M+1,$$
$$\frac{\left(\bar{a}^{\text{DL}}\right)^{\mathsf{H}} R_{kk}^{\text{DL}} \bar{a}^{\text{DL}} + \left| b_{kk}^{\text{DL}} \right|^2}{\sum_{l \neq k} \left(\bar{a}^{\text{DL}}\right)^{\mathsf{H}} R_{kl}^{\text{DL}} \bar{a}^{\text{DL}} + \left| b_{kl}^{\text{DL}} \right|^2 + \sigma_k^2} \geq \gamma_k, \forall k. (26)$$

The phase-shift matrix Θ^{DL} can be recovered from $\bar{a}^{\text{DL}}$ as follows. After solving problem (26) and obtaining a feasible solution $\bar{a}^{\text{DL}} = \left[a_0^{\text{DL}} \ t_0^{\text{DL}} \right]^{\mathsf{T}}$, the solution to problem (25) can be computed as $a^{\text{DL}} = a_0^{\text{DL}}/t_0^{\text{DL}}$, and the solution to $\mathscr{P}_2$ is given as $\Theta^{\text{DL}} = \beta \text{diag} \left(\left(a^{\text{DL}}\right)^{\mathsf{H}} \right)$.

C. Optimizing Variable Θ^{UL}

As Θ^{UL} does not appear in the objective function of $\mathscr{P}$, given $\mathcal{B}_1$ and $\mathcal{B}_2$, the resulting problem denoted as $\mathscr{P}_3$ is also a feasibility detection problem

$$\mathscr{P}_3: \quad \text{find} \quad \Theta^{\mathrm{UL}}$$
$$\text{subject to} \quad (13\mathrm{b}), (13\mathrm{f}).$$

The same derivation process presented in the last subsection is also applicable to transform the uplink problem $\mathscr{P}_3$ into a homogeneous QCQP, therefore details are omitted here for brevity. Specifically, by defining

$$\boldsymbol{w}_{nkl}^{\mathrm{UL}} = \beta \mathrm{diag}\left(\left(\boldsymbol{h}_{\mathrm{r},l}^{\mathrm{UL}}\right)^{\mathsf{H}}\right) \boldsymbol{G}_n^{\mathrm{UL}} \boldsymbol{v}_{nk}^{\mathrm{UL}}, \quad b_{nkl} = \left(\boldsymbol{h}_{\mathrm{d},nl}^{\mathrm{UL}}\right)^{\mathsf{H}} \boldsymbol{v}_{nk}^{\mathrm{UL}},$$

$$\boldsymbol{R}_{nkl}^{\mathrm{UL}} = \begin{bmatrix} \boldsymbol{w}_{nkl}^{\mathrm{UL}} \left(\boldsymbol{w}_{nkl}^{\mathrm{UL}}\right)^{\mathsf{H}} & \boldsymbol{w}_{nkl}^{\mathrm{UL}} \left(b_{nkl}^{\mathrm{UL}}\right)^{\mathsf{H}} \\ \left(\boldsymbol{w}_{nkl}^{\mathrm{UL}}\right)^{\mathsf{H}} b_{nkl}^{\mathrm{UL}} & 0 \end{bmatrix}, \quad \bar{\boldsymbol{a}}^{\mathrm{UL}} = \begin{bmatrix} \boldsymbol{a}^{\mathrm{UL}} \\ t^{\mathrm{UL}} \end{bmatrix},$$

we have the following uplink homogeneous QCQP problem

$$\text{find} \quad \bar{\boldsymbol{a}}^{\mathrm{UL}}$$
$$\text{subject to} \quad \left|\bar{a}_m^{\mathrm{UL}}\right|^2 = 1, \quad \text{for } m = 1, \dots, M+1,$$
$$\frac{p_k^{\mathrm{UL}}\left(\left(\bar{\boldsymbol{a}}^{\mathrm{UL}}\right)^{\mathsf{H}} \boldsymbol{R}_{nkk}^{\mathrm{UL}} \bar{\boldsymbol{a}}^{\mathrm{UL}} + \left|b_{nkk}^{\mathrm{UL}}\right|^2\right)}{\sum_{l \neq k} p_l^{\mathrm{UL}}\left(\left(\bar{\boldsymbol{a}}^{\mathrm{UL}}\right)^{\mathsf{H}} \boldsymbol{R}_{nkl}^{\mathrm{UL}} \bar{\boldsymbol{a}}^{\mathrm{UL}} + \left|b_{nkl}^{\mathrm{UL}}\right|^2\right) + \sigma_n^2 \left\|\boldsymbol{v}_{nk}^{\mathrm{UL}}\right\|_2^2} \geq \gamma_k,$$
$$\forall n, \forall k. \quad (27)$$

D. A Unified BSO Approach

Based on the above discussions, problem $\mathscr{P}$ is solved by iteratively solving problems $\mathscr{P}_1$, $\mathscr{P}_2$, and $\mathscr{P}_3$ in an alternating manner until convergence. We justify the effectiveness and depict the convergence behavior of the proposed BSO approach in the following proposition.

Proposition 1. *With the BSO approach, the objective value of $\mathscr{P}_1$ is non-increasing in the consecutive iterations.*

Proof. For ease of notation, we denote the objective value of $\mathscr{P}_1$ as $f(\boldsymbol{V}, \boldsymbol{\Omega})$, where the first variable $\boldsymbol{V}$ is an abstraction of three optimization variables $\{\boldsymbol{v}_{nk}^{\mathrm{DL}}\}$, $\{\boldsymbol{v}_{nk}^{\mathrm{UL}}\}$, and $\{p_k^{\mathrm{UL}}\}$ in $\mathscr{P}_1$, and the second variable $\boldsymbol{\Omega}$ abstracts phase-shift matrices $\boldsymbol{\Theta}^{\mathrm{DL}}$ and $\boldsymbol{\Theta}^{\mathrm{UL}}$ in $\mathscr{P}_2$ and $\mathscr{P}_3$. Assuming that $(\boldsymbol{V}^{(t)}, \boldsymbol{\Omega}^{(t)})$ is obtained at iteration t. If $\mathscr{P}_2$ and $\mathscr{P}_3$ are feasible, i.e., $(\boldsymbol{V}^{(t)}, \boldsymbol{\Omega}^{(t+1)})$ exists, $(\boldsymbol{V}^{(t)}, \boldsymbol{\Omega}^{(t+1)})$ is also feasible to $\mathscr{P}_1$. Therefore, $(\boldsymbol{V}^{(t)}, \boldsymbol{\Omega}^{(t)})$ and $(\boldsymbol{V}^{(t+1)}, \boldsymbol{\Omega}^{(t+1)})$ are feasible solutions to $\mathscr{P}_1$ at the consecutive iterations t and $t+1$, respectively. We have the following inequality

$$f(\boldsymbol{V}^{(t+1)}, \boldsymbol{\Omega}^{(t+1)}) \overset{(a)}{\leq} f(\boldsymbol{V}^{(t)}, \boldsymbol{\Omega}^{(t+1)}) \overset{(b)}{=} f(\boldsymbol{V}^{(t)}, \boldsymbol{\Omega}^{(t)}),$$

where (a) holds because $\boldsymbol{V}^{(t+1)}$ is the optimal solution to $\mathscr{P}_1$ for a given $\boldsymbol{\Omega}^{(t+1)}$ at iteration $t+1$, and (b) holds because the objective value P_{total} depends only on the value of $\boldsymbol{V}$ and is independent of $\boldsymbol{\Omega}$. $\square$

Although the BSO addresses the challenge of coupled optimization variables, problems (22), (26), and (27) are still intractable due to the non-convexity of these problems. In the next section, we shall propose effective algorithms to solve these nonconvex problems.

IV. BSO WITH MIXED $\ell_{1,2}$-NORM AND DC BASED THREE-STAGE FRAMEWORK FOR NETWORK POWER MINIMIZATION PROBLEM

In this section, we first propose two tractable algorithms for problems (22), (26), and (27), based on the mixed $\ell_{1,2}$ sparsity inducing norm and DC approach, respectively. Following these two algorithms, a three-stage framework is developed for problem $\mathscr{P}_{\mathrm{original}}$.

A. Mixed $\ell_{1,2}$-Norm for Group Sparsity Inducing

Although the feasible set is convex, problem (22) is a nonconvex integer programming problem due to the indicator function in the objective function. We identify that the third term in the objective function of problem (22) is a weighted ℓ_0-norm of vector $\bar{\boldsymbol{v}} = \left[\bar{\boldsymbol{v}}_{11}^{\mathsf{T}}, \bar{\boldsymbol{v}}_{12}^{\mathsf{T}}, \dots, \bar{\boldsymbol{v}}_{NK}^{\mathsf{T}}\right]^{\mathsf{T}}$ with weights $\{P_{nk}^{\mathsf{c}}, n \in \mathcal{N}\, k \in \mathcal{K}\}$, and it is non-convex. As ℓ_1-norm is a well-known convex relaxation to ℓ_0-norm, we relax the weighted ℓ_0-norm as

$$\sum_{n=1}^N \sum_{k=1}^K \mathbf{1}_{\{\bar{\boldsymbol{v}}_{nk}=\mathbf{0}\}} P_{nk}^{\mathsf{c}} \approx \sum_{n=1}^N \sum_{k=1}^K \|\bar{\boldsymbol{v}}_{nk}\|_2 \, P_{nk}^{\mathsf{c}}$$
$$= \sum_{n=1}^N \sum_{k=1}^K \sqrt{\|\boldsymbol{v}_{nk}^{\mathrm{DL}}\|_2^2 + \|\boldsymbol{v}_{nk}^{\mathrm{VDL}}\|_2^2} P_{nk}^{\mathsf{c}}. \quad (28)$$

Note that (28) is actually the weighted mixed $\ell_{1,2}$-norm of vector $\bar{\boldsymbol{v}}$. The mixed $\ell_{1,2}$-norm behaves like an ℓ_1-norm on vector $[\|\bar{\boldsymbol{v}}_{11}\|_2, \|\bar{\boldsymbol{v}}_{12}\|_2, \dots, \|\bar{\boldsymbol{v}}_{NK}\|_2]$. The outer ℓ_1-norm induces the sparsity structure, while the inner ℓ_2-norm is responsible for forcing all coefficients in the beamforming group $\bar{\boldsymbol{v}}_{nk}$ to be zero. By adopting mixed $\ell_{1,2}$-norm as the convex relaxation of the indicator function term, we can induce the group sparsity structure of beamforming groups $\{\bar{\boldsymbol{v}}_{nk}, n \in \mathcal{N}, k \in \mathcal{K}\}$.

Remark: In general, all the mixed $\ell_{1,p}$-norm with $p \geq 1$ can induce the group sparsity structure [42]. However for brevity, we adopt the most commonly used mixed $\ell_{1,2}$-norm in this paper.

By replacing the indication function with its convex surrogate, we relax problem (22) as the following convex problem

$$\underset{\{\boldsymbol{v}_{nk}^{\mathrm{DL}}\}, \{\boldsymbol{v}_{nk}^{\mathrm{VDL}}\}}{\text{minimize}} \quad \sum_{n=1}^N \sum_{k=1}^K \|\boldsymbol{v}_{nk}^{\mathrm{VDL}}\|_2^2 + \sum_{n=1}^N \sum_{k=1}^K \frac{1}{\eta_n} \|\boldsymbol{v}_{nk}^{\mathrm{DL}}\|_2^2$$
$$+ \sum_{n=1}^N \sum_{k=1}^K \sqrt{\|\boldsymbol{v}_{nk}^{\mathrm{DL}}\|_2^2 + \|\boldsymbol{v}_{nk}^{\mathrm{VDL}}\|_2^2} P_{nk}^{\mathsf{c}}$$
$$\text{subject to} \quad (13\mathrm{c}), (14), (19), (21). \quad (29)$$

As we have discussed in Section III-A, the solutions to the non-convex problem $\mathscr{P}_1$ can be obtained by utilizing the solutions to problem (29). The overall algorithm for solving problem $\mathscr{P}_1$ is summarized in Algorithm 1.

As problem $\mathscr{P}_{1\text{-}2}$ with fixed $\{\boldsymbol{v}_{nk}^{\mathrm{UL}}\}$ can be efficiently solved by the fixed-point iterations [38], the computational complexity of Algorithm 1 is dominated by solving the SOCP problem (29), which is $\mathcal{O}(L^{3.5}K^{3.5})$ using interior-point methods [43].

Algorithm 1: Mixed $\ell_{1,2}$-Norm Based Group Sparsity Inducing for Problem $\mathscr{P}_1$

Input: $\Theta^{\mathrm{UL}}, \Theta^{\mathrm{DL}}$

1. solve the convex relaxation problem (29) to obtain $\{v_{nk}^{\mathrm{DL}}\}, \{v_{nk}^{\mathrm{VDL}}\}$
2. set $v_{nk}^{\mathrm{UL}} = v_{nk}^{\mathrm{VDL}}, \forall n \in \mathcal{N}, k \in \mathcal{K}$, and then solve problem $\mathscr{P}_{1\text{-}2}$ with fixed $\{v_{nk}^{\mathrm{UL}}\}$ to obtain $\{p_k^{\mathrm{UL}}\}$

Output: $\{v_{nk}^{\mathrm{DL}}\}, \{v_{nk}^{\mathrm{UL}}\}, \{p_k^{\mathrm{UL}}\}$

B. DC Approach for Nonconvex QCQP Problem

The non-convexity of problems (26) and (27) lie in the unit-modulus constraints. A common technique used to handle the nonconvex QCQP problems is matrix lifting. For ease of notation, we omit the superscripts DL and UL if it does not cause any ambiguity. In problem (26), as $\bar{a}^{\mathsf{H}} R_{kk} \bar{a} = \mathrm{Tr}\left(R_{kk}\bar{a}\bar{a}^{\mathsf{H}}\right)$, and by introducing a new variable $A = \bar{a}\bar{a}^{\mathsf{H}} \in \mathbb{C}^{(M+1)\times(M+1)}$, we rewrite problem (26) as the following feasibility detection problem

$$\text{find} \quad A$$

$$\text{subject to} \quad \mathrm{Tr}\left(R_{kk}A\right) + |b_{kk}|^2 \geq \gamma_k \sum_{l \neq k}^{K} \mathrm{Tr}\left(R_{kl}A\right)$$

$$+ \gamma_k \left(\sum_{l \neq k}^{K} |b_{kl}|^2 + \sigma_k^2\right), \forall k, \quad (30a)$$

$$A_{mm} = 1, \text{for } m = 1, \ldots, M+1, \quad (30b)$$

$$A \succeq 0, \ \mathrm{rank}(A) = 1. \quad (30c)$$

Here $A \succeq 0$ indicates that A is a positive semidefinite (PSD) matrix. The challenge in solving problem (30) is the nonconvex rank-one constraint. Semidefinite relaxation (SDR) technique is widely adopted to tackle the rank-one constraint in QCQP problems [44]. By simply dropping the nonconvex rank-one constraint, SDR relaxes the problem into a convex semidefinite programming (SDP) problem, which can then be solved by CVX. If a feasible A with rank one is found, then $\bar{a}$ can be obtained by singular value decomposition (SVD) of A.

However, such a relaxation may not be tight, i.e., the solution obtained by SDR may not satisfy the rank-one constraint. As pointed out in [45], [46], the performance of SDR degrades sharply as the problem size grows. In our case, when M and/or K is large, the probability of returning a rank-one solution is low. If this is the case, additional steps (i.e., Gaussian randomization) are required to construct a rank-one solution from the higher-rank solution obtained by solving problem (30) [19], [44]. However, it is still possible that we fail to find a feasible solution to problem (26) after a large number of Gaussian randomizations.

In other words, dropping the rank-one constraint cannot accurately detect the feasibility of problem (30). Hence, we propose a novel DC representation for the rank-one constraint, which is capable of guaranteeing the feasibility of the nonconvex rank-one constraint and thus detecting the exact feasibility of problem (30). Note that for the PSD matrix A, the rank-one constraint indicates that

$$\sigma_1(A) > 0 \text{ and } \sigma_i(A) = 0, \ \forall i = 2, \ldots, M+1,$$

where $\sigma_i(A)$ is the i-th largest singular value of A. And recall that the trace norm and spectral norm of A are defined as

$$\mathrm{Tr}(A) = \sum_{i=1}^{M+1} \sigma_i(A) \ \text{ and } \ \|A\| = \sigma_1(M),$$

respectively. Hence, the rank-one constraint can be equivalently rewritten as the difference of these two convex norms, i.e.,

$$\mathrm{rank}(A) = 1 \iff \mathrm{Tr}(A) - \|A\| = 0, \ \mathrm{Tr}(A) > 0. \quad (31)$$

Based on the DC representation for the nonconvex rank-one constraint, problem (30) is reformulated as follows

$$\underset{A \succeq 0}{\text{minimize}} \quad g(A) := \mathrm{Tr}(A) - \|A\|$$

$$\text{subject to} \quad (30a) - (30b). \quad (32)$$

The rank-one constraint is satisfied when the objective value $g(A)$ becomes zero. Although problem (32) is still nonconvex due to the concave term $-\|A\|$ in the objective, we can derive a DC algorithm to solve it in an iterative manner. Specifically, by linearizing the concave term, at iteration i we need to solve the following convex problem

$$\underset{A \succeq 0}{\text{minimize}} \quad \mathrm{Tr}(A) - \left\langle \partial\|A^{[i-1]}\|, A \right\rangle$$

$$\text{subject to} \quad (30a) - (30b). \quad (33)$$

where $A^{[i-1]}$ is the solution obtained at iteration $i-1$ and $\partial\|A^{[i-1]}\|$ denotes the subgradient of spectral norm at point $A^{[i-1]}$. Note that one subgradient of $\|A\|$ can be efficiently computed as $q_1 q_1^{\mathsf{H}}$, where q_1 is the vector corresponding to the largest singular value $\sigma_1(A)$ [47]. By iteratively solving (33) until the objective function $g(A)$ in (32) becomes zero, we obtain an exact rank-one solution according to (31). We design a practical stopping criterion as $\mathrm{Tr}(A) - \|A\| < \epsilon_{DC}$, where ϵ_{DC} is a sufficiently small positive constant.

The convergence characteristic of the iterative DC algorithm for problem (32) is presented in the following proposition.

Proposition 2. *The generated sequence $\{g(A^{[i]})\}$ is strictly decreasing and the sequence $\{A^{[i]}\}$ converges to a critical point of g from an arbitrary initial point $A^{[0]}$.*

Proof. Please refer to [46, Appendix B] for more details. $\square$

The proposed DC algorithm can always accurately detect the feasibility of problem (30) by obtaining a feasible A, which guarantees the optimal objective value of problem (32) is zero. This is because the feasible region of problem (30) is always non-empty, at least the obtained solution to problem (30) at iteration t (i.e., $\Theta^{(t)}$) is still feasible at iteration $t+1$. Therefore, the strictly decreasing and non-negative sequence $\{g(A^{[i]})\}$ can always converge to zero within finite steps.

Similarly, we can lift the uplink counterpart (27) as the following feasibility detection problem

$$\text{find} \quad \boldsymbol{A}$$

$$\text{subject to} \quad \text{Tr}\left(\boldsymbol{R}_{nkk}\boldsymbol{A}\right) + |b_{nkk}|^2 \geq \gamma_k \sum_{l \neq k}^{K} \alpha_{kl} \text{Tr}\left(\boldsymbol{R}_{nkl}\boldsymbol{A}\right)$$

$$+ \gamma_k \left(\sum_{l \neq k}^{K} \alpha_{kl} |b_{nkl}|^2 + c_{nk} \right), \quad \forall n, \forall k, \text{(34a)}$$

$$\boldsymbol{A}_{mm} = 1, \text{for } m = 1, \ldots, M+1, \quad \text{(34b)}$$

$$\boldsymbol{A} \succeq \boldsymbol{0}, \ \text{rank}(\boldsymbol{A}) = 1, \quad \text{(34c)}$$

where $\alpha_{kl} = p_l^{\text{UL}}/p_k^{\text{UL}}$ and $c_{nk} = \sigma_n^2 \|\boldsymbol{v}_{nk}^{\text{UL}}\|_2^2 /p_k^{\text{UL}}$, and iteratively solve the following DC program

$$\underset{\boldsymbol{A} \succeq \boldsymbol{0}}{\text{minimize}} \quad \text{Tr}(\boldsymbol{A}) - \left\langle \partial\|\boldsymbol{A}^{[i-1]}\|, \boldsymbol{A} \right\rangle$$

$$\text{subject to} \quad \text{(34a)} - \text{(34b)}. \quad \text{(35)}$$

until the stopping criterion is satisfied to obtain a feasible solution to problem (34).

The overall algorithm for solving problem $\mathscr{P}_2$ (or $\mathscr{P}_3$) is summarized in Algorithm 2. The complexity of Algorithm 2 is dominated by iteratively solving the SDP problem (33) (or problem (35)) and computing the subgradient of $\boldsymbol{A}$. In each iteration, problem (33) is solved with complexity $\mathcal{O}(KM^3)$ (or $\mathcal{O}(NKM^3)$ for problem (35)) using interior-point methods [43], while the subgradient can be computed by SVD with complexity $\mathcal{O}(M^3)$. Furthermore, it is observed in our simulations that the convergence rate of the iterative procedure is fast (less than 10 iterations), therefore the overall complexity of Algorithm 2 is at most $\mathcal{O}\left(NKM^3\right)$.

Algorithm 2: DC Algorithm for Feasibility Detection Problem $\mathscr{P}_2$ (or $\mathscr{P}_3$)

Input: $\{\boldsymbol{v}_{nk}^{\text{DL}}\}, \{\boldsymbol{v}_{nk}^{\text{VDL}}\}, \{p_k^{\text{UL}}\}$ and initial point $\boldsymbol{A}^{[0]}$
1. iteratively solve problem (33) (or problem (35)) until the stopping criterion $\text{Tr}(\boldsymbol{A}) - \|\boldsymbol{A}\| < \epsilon_{DC}$ is satisfied
2. decompose $\boldsymbol{A}$ as $\boldsymbol{A} = \bar{\boldsymbol{a}}\bar{\boldsymbol{a}}^{\text{H}}$; denote $\bar{\boldsymbol{a}} = [\boldsymbol{a}_0, t_0]^{\text{T}}$; then we obtain $\boldsymbol{a} = \boldsymbol{a}_0/t_0$ and $\boldsymbol{\Theta} = \beta\text{diag}\left(\boldsymbol{a}^{\text{H}}\right)$
Output: $\boldsymbol{\Theta}^{\text{UL}}$ (or $\boldsymbol{\Theta}^{\text{DL}}$)

C. A Three-Stage Framework for Green Edge Inference

In this subsection, we propose a thorough three-stage framework for the green edge inference problem $\mathscr{P}_{\text{original}}$. In the first stage, we adopt the BSO with mixed $\ell_{1,2}$-norm and DC algorithm to induce the group sparsity structure of uplink/downlink beamforming vectors and optimize the phase-shift matrices. The obtained solutions serve as a guideline to determine the inference task selection strategy $\mathcal{A}$. In the second stage, an ordering rule is proposed for all tasks according to their priorities, which depend on the structured-sparse beamforming vectors obtained in the first stage as well as several key system parameters (i.e., channel state information, amplifier efficiency and task computation power). Based on the task ordering, we perform a task selection procedure to finalize

$\mathcal{A}$. In the last stage, the beamforming vectors and phase-shift matrices are refined with the finalized task selection strategy $\mathcal{A}$.

Stage 1. Group Sparsity Inducing: With randomly initialized phase-shift matrices $\boldsymbol{\Theta}^{\text{UL}}$ and $\boldsymbol{\Theta}^{\text{DL}}$, we repeatedly solve problems $\mathscr{P}_1$, $\mathscr{P}_2$, and $\mathscr{P}_3$ based on Algorithms 1 and 2 respectively in an alternating manner until the following stopping criterion is satisfied: the relative improvement of objective values of problem $\mathscr{P}_1$ defined as $\left(P_{\text{total}}^{(t)} - P_{\text{total}}^{(t+1)}\right)/P_{\text{total}}^{(t)}$ is below a predefined threshold ε, where $P_{\text{total}}^{(t)}$ and $P_{\text{total}}^{(t+1)}$ represent the objective values obtained in iterations t and $t+1$, respectively. The yielded beamforming vectors should have the group sparsity structures. It is worth mentioning that the relative improvement is expected to be non-negative, because P_{total} is non-increasing as proved in Proposition 1.

Stage 2. Inference Task Selection: The next question is how to determine the task selection strategy $\mathcal{A}$. In fact, it is inappropriate to directly use the beamforming vectors obtained in *Stage 1* to finalize $\mathcal{A}$, as the vectors may contain some very small but nonzero coefficients. As illustrated in (11), these nonzero coefficients indicate that the corresponding tasks are performed by the BSs, which may result in unnecessary computation power consumption. To address this issue, we utilize the obtained group-structured beamforming vectors as well as other prior information to provide a guideline to determine set $\mathcal{A}$.

For ease of exposition, we define the set of all task indices as $\{(n,k)|n \in \mathcal{N}, \ k \in \mathcal{K}\}$. The task indexed by (n,k) is considered to be *active* if $k \in \mathcal{A}_n$, and *inactive* otherwise. Specifically, the priority of task (n,k) is defined as

$$\tau_{nk} = \sqrt{\frac{\left\|\left[\boldsymbol{g}_{nk}^{\text{UL}}, \boldsymbol{g}_{nk}^{\text{DL}}\right]\right\|_2^2 \eta_n}{P_{nk}^{\text{c}}}} \|\boldsymbol{v}_{nk}\|_2. \quad \text{(36)}$$

We sort all NK tasks in a descending order according to their priorities, i.e., $\tau_{\pi_1} \geq \tau_{\pi_2} \cdots \geq \tau_{\pi_{NK}}$, where π is a permutation of task indices (n,k)'s. Intuitively, if BS n has a higher power amplifier efficiency, a higher channel gain, and a higher beamforming gain with respect to MD k, but lower computation power consumption, task (n,k) has a higher priority. A higher τ_{nk} implies that task (n,k) is more power-efficient, therefore it is more likely to be activated.

To finalize the task selection strategy, we need to detect the feasibility of a sequence of problems

$$\text{find} \quad \{\boldsymbol{v}_{nk}^{\text{DL}}\}, \{\boldsymbol{v}_{nk}^{\text{UL}}\}, \{p_k^{\text{UL}}\}$$

$$\text{subject to} \quad \text{(13a)} - \text{(13d)},$$

$$\boldsymbol{v}_{\pi^{[j]}} = \boldsymbol{0}, \quad \text{(37)}$$

where $\pi^{[j]} = \{\pi_{j+1}, \ldots, \pi_{NK}\}$ denotes the inactive task set at iteration j, and $\boldsymbol{v}_{\pi^{[j]}} = \boldsymbol{0}$ represents that all coefficients in those beamforming groups $\boldsymbol{v}_{nk}$'s with index $(n,k) \in \pi^{[j]}$ are set to zero. Note that the number of active tasks is within $[K, NK]$. Starting with $j = K$, we terminate the feasibility detection procedure and return $\pi^{[j]}$ until problem (37) is feasible. The task selection strategy $\mathcal{A}$ can be easily obtained from $\pi^{[j]}$.

Comparing problem (37) to $\mathscr{P}_1$, as the added constraint $\boldsymbol{v}_{\pi[j]} = \boldsymbol{0}$ is convex, we can solve problem (37) using Algorithm 1. Details are thus omitted here for brevity.

Stage 3. Optimization Variables Refinement: After determining the task selection strategy $\mathcal{A}$, the computation power $\sum_{n \in \mathcal{N}} \sum_{k \in \mathcal{A}_n} P_{nk}^{\mathrm{c}}$ is a constant and can be removed from the objective function. The uplink receive beamforming vectors and downlink transmit beamforming vectors are determined by coordinated beamforming among the BSs, and the phase-shift matrices at the RIS need to be refined as well. We solve the following problem to refine these optimization variables

$$\underset{\{\boldsymbol{v}_{nk}^{\mathrm{DL}}\},\{\boldsymbol{v}_{nk}^{\mathrm{UL}}\},\{p_k^{\mathrm{UL}}\},\boldsymbol{\Theta}^{\mathrm{DL}},\boldsymbol{\Theta}^{\mathrm{UL}}}{\text{minimize}} \quad \sum_{k=1}^{K} p_k^{\mathrm{UL}} + \sum_{n=1}^{N} \sum_{k=1}^{K} \frac{1}{\eta_n} \|\boldsymbol{v}_{nk}^{\mathrm{DL}}\|_2^2$$
$$\text{subject to} \quad (13a) - (13f),$$
$$\boldsymbol{v}_{\pi[j]} = \boldsymbol{0}. \tag{38}$$

Comparing problem (38) to $\mathscr{P}$, since the added constraint $\boldsymbol{v}_{\pi[j]} = \boldsymbol{0}$ is convex, the BSO with mixed $\ell_{1,2}$-norm and DC algorithm to solve problem $\mathscr{P}$ is also applicable here to obtain the solutions. Details are thus omitted here.

The overall algorithm for green edge inference is summarized in Algorithm 3. By denoting the required iterations for the BSO to converge as T, the computational complexity involved in *Stage 1* is $\mathcal{O}\left(T(L^{3.5}K^{3.5} + NKM^3)\right)$, where $\mathcal{O}(L^{3.5}K^{3.5} + NKM^3)$ is the complexity at each iteration discussed in Sections IV-A and IV-B. We need to solve a sequence of SOCP problems in *Stage 2*, and hence the worst-case complexity is $\mathcal{O}\left(NK(L^{3.5}K^{3.5})\right)$. The complexity involved in *Stage 3* is the same as that in *Stage 1*. Therefore, the overall complexity for the proposed three-stage framework is $\mathcal{O}\left(T(L^{3.5}K^{3.5} + NKM^3) + NL^{3.5}K^{4.5}\right)$.

Algorithm 3: BSO with Mixed $\ell_{1,2}$-Norm and DC Based Three-Stage Framework for Nonconvex Combinatorial Problem $\mathscr{P}_{\mathrm{original}}$

Input: initial phase-shift matrices $\boldsymbol{\Theta}^{\mathrm{UL}}$ and $\boldsymbol{\Theta}^{\mathrm{DL}}$, and threshold ε

Stage 1: Alternatively optimize $\mathcal{B}_1$, $\mathcal{B}_2$, and $\mathcal{B}_3$

while *the improvement of the objective in problem $\mathscr{P}_1$ is greater than ε* **do**

    1. solve $\mathscr{P}_1$ for $\boldsymbol{v}_{nk}^{\mathrm{UL}}, p_k^{\mathrm{UL}}, \boldsymbol{v}_{nk}^{\mathrm{DL}}$ using Algorithm 1
    2. solve $\mathscr{P}_2$ for $\boldsymbol{\Theta}^{\mathrm{DL}}$ using Algorithm 2
    3. solve $\mathscr{P}_3$ for $\boldsymbol{\Theta}^{\mathrm{UL}}$ using Algorithm 2

end

Stage 2: Determine the inference task selection

1. compute task priorities based on (36) and sort all tasks in a descending order according to their priorities
2. iteratively solve problem (37) until feasible to finalize the task selection strategy $\mathcal{A}$

Stage 3: Solve problem (38) to refine variables $\{\boldsymbol{v}_{nk}^{\mathrm{DL}}\}, \{\boldsymbol{v}_{nk}^{\mathrm{UL}}\}, \{p_k^{\mathrm{UL}}\}, \boldsymbol{\Theta}^{\mathrm{DL}}, \boldsymbol{\Theta}^{\mathrm{UL}}$

Output: $\mathcal{A}, \{\boldsymbol{v}_{nk}^{\mathrm{DL}}\}, \{\boldsymbol{v}_{nk}^{\mathrm{UL}}\}, \{p_k^{\mathrm{UL}}\}, \boldsymbol{\Theta}^{\mathrm{DL}}, \boldsymbol{\Theta}^{\mathrm{UL}}$

V. SIMULATION RESULTS

In this section, we present the simulation results to verify the effectiveness of our proposed algorithm. We consider a network with five 8-antenna BSs and six MDs uniformly and independently distributed in a square region of $300\,\mathrm{m} \times 300\,\mathrm{m}$. An RIS with 30 reflecting elements is located at the 3-dimensional coordinate $(150, 0, 20)$. In addition, the BSs are with height $30\,\mathrm{m}$ (i.e., the coordinates of the BSs are $(x, y, 30)$), while the MDs are with height $0\,\mathrm{m}$ (i.e., the coordinates of the MDs are $(x, y, 0)$).

We consider the following distance-dependent path loss model $L(d) = T_0 \left(\frac{d}{d_0}\right)^{-\alpha}$, where T_0 is the constant path loss at the reference distance d_0, d is the Euclidean distance between the transceivers, and α is the path loss exponent. Each antenna of the BSs is assumed to have an isotropic radiation pattern (i.e., $0\,\mathrm{dBi}$ antenna gain), while each element of the RIS has a $3\,\mathrm{dBi}$ gain because it reflects signals only in its front half-space [26], [48]. Moreover, Rayleigh fading is considered as the small-scale fading model for all channels. Specifically, the channel coefficients are given by $\boldsymbol{h}_{\mathrm{d},nk}^x = \sqrt{L(d_{\mathrm{BU}})}\boldsymbol{\xi}_1$, $\boldsymbol{G}_n^x = \sqrt{10^{0.3}L(d_{\mathrm{RB}})}\boldsymbol{\Gamma}$, and $\boldsymbol{h}_{\mathrm{r},k}^x = \sqrt{10^{0.3}L(d_{\mathrm{RU}})}\boldsymbol{\xi}_2$, where $\boldsymbol{\xi}_1, \boldsymbol{\xi}_2 \sim \mathcal{CN}(\boldsymbol{0}, \boldsymbol{I})$, $\boldsymbol{\Gamma} \sim \mathcal{CN}(\boldsymbol{0}, \boldsymbol{I})$, and superscript $x \in \{\mathrm{UL}, \mathrm{DL}\}$. Without specified otherwise, we set $T_0 = -10\,\mathrm{dB}$, $d_0 = 1\,\mathrm{m}$, $P_{n,\max}^{\mathrm{DL}} = 1\,\mathrm{W}$, $P_{n,\max}^{\mathrm{UL}} = 1\,\mathrm{W}$, $P_{nk}^{\mathrm{c}} = 0.45\,\mathrm{W}$, $\sigma_k^2 = -53\,\mathrm{dBm}$, $\sigma_n^2 = -63\,\mathrm{dBm}$, $\eta_n = 0.25$, $\beta = 1$, $\epsilon_{DC} = 10^{-6}$, $\varepsilon = 10^{-2}$, and $\gamma_k^{\mathrm{UL}} = \frac{1}{2}\gamma_k^{\mathrm{DL}}$. The path loss exponent α is set as $2, 3.5$, and 2.5 for BS-RIS channel, BS-MD channel, and RIS-MD channel, respectively.

We compare the proposed BSO with mixed $\ell_{1,2}$-norm and DC algorithm (abbreviated as BSO-$\ell_{1,2}$-DC) with the following benchmarks.

- **Without-RIS**: Without the deployment of an RIS, the equivalent channels in (2) and (6) contain only the direct link, i.e., $\boldsymbol{h}_{\mathrm{r},k}^{\mathrm{UL}} = \boldsymbol{h}_{\mathrm{r},k}^{\mathrm{DL}} = \boldsymbol{0}, \forall k$. As we do not need to optimize phase shifts in this case, the alternating process in *Stage 1* is simplified to solve $\mathscr{P}_1$ only once.

- **BSO with mixed $\ell_{1,2}$-norm and Random Phase** (abbreviated as BSO-$\ell_{1,2}$-RP): In this case, the phase shifts of all reflecting elements in both uplink and downlink transmissions are randomly chosen from $[0, 2\pi)$ and then used to solve problem $\mathscr{P}_1$. We do not solve problems $\mathscr{P}_2$ and $\mathscr{P}_3$ in *Stage 1* subsequently to optimize the phase shifts. This benchmark is designed to reveal the necessity of optimizing the phase-shift matrices.

- **BSO with mixed $\ell_{1,2}$-norm and SDR** (abbreviated as BSO-$\ell_{1,2}$-SDR): In this case, the nonconvex rank-one constraints in (30) and (34) are dropped. Gaussian randomization is then adopted to obtain a feasible solution to problems $\mathscr{P}_2$ and $\mathscr{P}_3$. The number of randomly generated vectors for Gaussian randomization is set as 500. If Gaussian randomization fails to find a feasible solution, we terminate the alternating process in *Stage 1*.

A. Effectiveness of Deploying An RIS

In this subsection, we compare our RIS-aided communication system with the conventional one without the assistance of

TABLE I: Feasible Probability versus Target SINR

Target SINR [dB]	-20	-15	-10	-5	0	5	10
Without-RIS	1.00	0.84	0.48	0.08	0	0	0
BSO-$\ell_{1,2}$-RP	**1.00**	**1.00**	**1.00**	**1.00**	**0.97**	**0.84**	**0.42**

TABLE II: Overall Power Consumption versus Target SINR

Target SINR [dB]	-20	-15	-10	-5	0	5	10
Without-RIS [W]	3.04	3.52	5.17	9.60	N/A	N/A	N/A
BSO-$\ell_{1,2}$-RP [W]	**3.02**	**3.12**	**3.32**	**3.75**	**4.72**	**7.66**	**14.79**
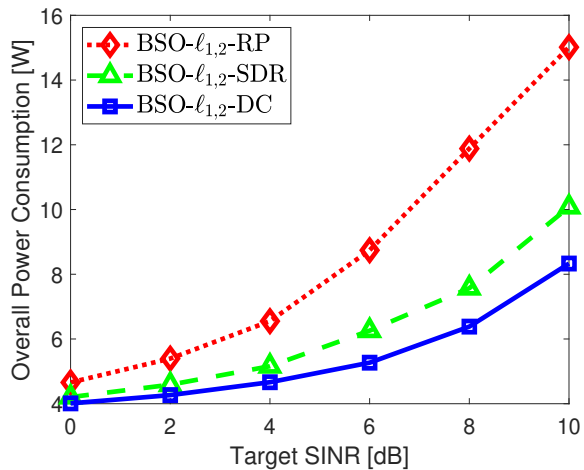
Fig. 2: The overall network power consumption versus target SINR γ_k^{DL}.

an RIS. For fair comparison, we do not explicitly optimize the phase-shift matrices, i.e., we compare the performance of Without-RIS and BSO-$\ell_{1,2}$-RP.

We first study the relationship between the feasible probability of problem $\mathscr{P}_{\text{original}}$ and the target SINR γ_k^{DL}. The feasible probability of problem $\mathscr{P}_{\text{original}}$ is defined as

$$\mathbb{P}\{\mathscr{P}_{\text{original}} \text{ is feasible}\} = \frac{\text{number of cases } \mathscr{P}_{\text{original}} \text{ is feasible}}{\text{number of total test cases}}.$$

As the target SINR requirements become more stringent, i.e., larger values of γ_k^{UL} and γ_k^{DL}, the feasibility probability of problem $\mathscr{P}_{\text{original}}$ is expected to decline. Results illustrated in Table I are averaged over 200 independently generated channel realizations. We can see that the conventional system without RIS fails to support those settings with a target SINR being higher than 0 dB, while the RIS-aided system can still support with a high probability. In terms of the maximum SINR that the communication systems can support, we observe that there exists at least a 15 dB gain of the RIS-aided system over the system without RIS.

Table II illustrates the overall network power consumption of systems with and without RIS. Under the same SINR requirement, it is observed that BSO-$\ell_{1,2}$-RP yields a significantly lower power consumption. The supreme performance gain demonstrates that the deployment of an RIS in wireless communication systems can greatly boost the SINR and in turn reduce the overall network power consumption.
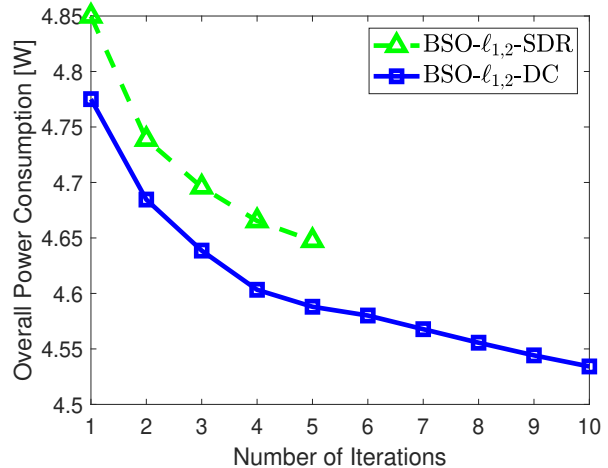
Fig. 3: Convergence behaviors of both BSO-$\ell_{1,2}$-DC and BSO-$\ell_{1,2}$-SDR algorithms.
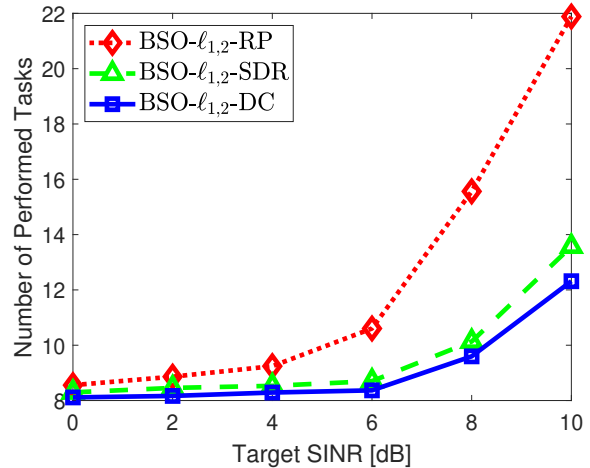
(a) Number of performed tasks versus target SINR.
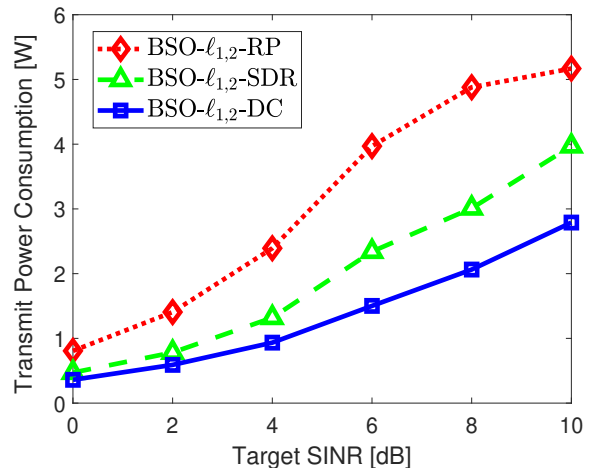
(b) Transmit power consumption versus target SINR.

Fig. 4: Different components of the overall network power consumption versus target SINR γ_k^{DL}.

B. Superiority of The Proposed BSO-$\ell_{1,2}$-DC Algorithm

In this subsection, we show the superiority of our proposed BSO-$\ell_{1,2}$-DC algorithm. The overall network power consumption shown in Fig. 2 is averaged over 150 independent channel realizations.

The first observation is that both the BSO-$\ell_{1,2}$-DC and BSO-$\ell_{1,2}$-SDR algorithms significantly outperform BSO-$\ell_{1,2}$-RP, which demonstrates that dynamically optimizing the phase-shift matrices according to the beamforming vectors can reduce the network power consumption to a large extent. In addition, we observe that the proposed BSO-$\ell_{1,2}$-DC algorithm yields a much lower overall network power consumption and is more energy efficient than the BSO-$\ell_{1,2}$-SDR algorithm. Given an overall power budget (e.g., 6 W), BSO-$\ell_{1,2}$-DC can achieve around 2 dB higher SINR for the MDs than BSO-$\ell_{1,2}$-SDR. Such a performance gain is mainly because BSO-$\ell_{1,2}$-SDR may early terminate the alternating BSO process in *Stage 1* and cannot further proceed to find feasible solutions to problems $\mathscr{P}_2$ and/or $\mathscr{P}_3$. To make this more explicit, Fig. 3 shows the objective values of problem $\mathscr{P}_1$ in the first 10 alternating iterations in a specific channel realization. It is observed that as the BSO approach proceeds, the overall network power consumption for both BSO-$\ell_{1,2}$-DC and BSO-$\ell_{1,2}$-SDR algorithms are non-increasing, which validates our analysis in Proposition 1. It is also observed that the BSO-$\ell_{1,2}$-SDR algorithm terminates at the 5th iteration, as SDR fails to obtain feasible solutions to problems $\mathscr{P}_2$ and/or $\mathscr{P}_3$ even with Gaussian randomization techniques. In contrast, DC can always yield feasible solutions as we have discussed in Section IV-B, and therefore BSO-$\ell_{1,2}$-DC terminates the alternating process only when the consecutive iterations make little progress.

Another interesting point worth mentioning in Fig. 2 is that the performance gaps between BSO-$\ell_{1,2}$-DC and other algorithms are getting larger as the value of the target SINR increases, which indicates that BSO-$\ell_{1,2}$-DC is especially appealing when high-quality services are required by the MDs. This is because a higher target SINR leads to a narrower feasible region of problems $\mathscr{P}_2$ and $\mathscr{P}_3$, making SDR less likely to find a feasible solution. In short, Fig. 2 shows that the proposed BSO-$\ell_{1,2}$-DC is able to reduce the overall network power consumption by 20% in the low SINR regime, and by up to 45% in the high SINR regime.

The number of tasks performed by all the BSs and the transmit power consumption versus the target SINR are shown in Fig. 4a and Fig. 4b, respectively. As the target SINR increases, both the number of performed tasks and transmit power consumption increase. It is observed in Fig. 4a that BSO-$\ell_{1,2}$-DC can always perform fewer tasks to satisfy a certain target SINR. In other words, the long-lasting alternating iterations of BSO-$\ell_{1,2}$-DC shown in Fig. 3 helps promote the group sparsity structure of beamforming vectors, thereby achieving lower computation power consumption. In terms of the transmit power consumption depicted in Fig. 4b, we make the similar observation that BSO-$\ell_{1,2}$-DC yields the lowest transmit power consumption. Finally, it is also observed that the performance gaps between BSO-$\ell_{1,2}$-DC and other algorithms tend to be larger in the high SINR regime.

VI. Conclusions

In this paper, we investigated an RIS-aided edge inference system with multiple BSs cooperatively serving multiple MDs, taking into account both uplink and downlink transmissions. The design of an energy-efficient edge inference system was formulated as a joint uplink and downlink beamforming, transmit power and phase-shift matrices design problem. A BSO approach was proposed to decouple the optimization variables. For efficient algorithm design, mixed $\ell_{1,2}$-norm was adopted to induce group sparsity of uplink/downlink beamforming vectors, while the matrix lifting and DC techniques were exploited to handle the nonconvex rank-one constraint and in turn solve the phase-shift matrix optimization problems. Through numerical simulations, we demonstrated that the deployment of an RIS significantly reduces the overall network power consumption. Furthermore, the effectiveness of DC algorithm for inducing low-rank solutions was verified. We also clarified the convergence behavior of the proposed BSO approach in this paper. For future work, we will study the precise convergence rate of the proposed algorithm.

References

[1] S. Hua and Y. Shi, "Reconfigurable intelligent surface for green edge inference in machine learning," in *Proc. IEEE Global Commun. Conf. (Globecom) Workshops*, Waikoloa, Hawaii, Dec. 2019.

[2] "Cisco visual networking index: Global mobile data traffic forecast update, 20172022," Available: https://www.cisco.com/c/en/us/solutions/collateral/service-provider/visual-networking-index-vni/white-paper-c11-738429.pdf, Feb. 2019.

[3] K. B. Letaief, W. Chen, Y. Shi, J. Zhang, and Y. A. Zhang, "The roadmap to 6G: AI empowered wireless networks," *IEEE Commun. Mag.*, vol. 57, no. 8, pp. 84–90, Aug. 2019.

[4] J. Chen and X. Ran, "Deep learning with edge computing: A review," *Proc. IEEE*, vol. 107, no. 8, pp. 1655–1674, Aug. 2019.

[5] J. Zhang and K. B. Letaief, "Mobile edge intelligence and computing for the internet of vehicles," *Proc. IEEE, early access*, 2019.

[6] S. Liu, Y. Lin, Z. Zhou, K. Nan, H. Liu, and J. Du, "On-demand deep model compression for mobile devices: A usage-driven model selection framework," *in Proc. ACM MobiSys*, pp. 389–400, Munich, Germany, Jun. 2018.

[7] B. Taylor, V. S. Marco, W. Wolff, Y. Elkhatib, and Z. Wang, "Adaptive deep learning model selection on embedded systems," *ACM SIGPLAN Notices*, vol. 53, no. 6, pp. 31–43, 2018.

[8] Z. Du, R. Fasthuber, T. Chen, P. Ienne, L. Li, T. Luo, X. Feng, Y. Chen, and O. Temam, "Shidiannao: Shifting vision processing closer to the sensor," *ACM SIGARCH Computer Architecture News*, vol. 43, no. 3, pp. 92–104, 2015.

[9] W. Shi, J. Cao, Q. Zhang, Y. Li, and L. Xu, "Edge computing: Vision and challenges," *IEEE Internet Things J.*, vol. 3, no. 5, pp. 637–646, Oct. 2016.

[10] Z. Zhou, X. Chen, E. Li, L. Zeng, K. Luo, and J. Zhang, "Edge intelligence: Paving the last mile of artificial intelligence with edge computing," *Proc. IEEE*, vol. 107, no. 8, pp. 1738–1762, Aug. 2019.

[11] E. Li, L. Zeng, Z. Zhou, and X. Chen, "Edge AI: On-demand accelerating deep neural network inference via edge computing," *IEEE Trans. Wireless Commun., early access*, 2019.

[12] C. Hu, W. Bao, D. Wang, and F. Liu, "Dynamic adaptive DNN surgery for inference acceleration on the edge," in *Proc. IEEE INFOCOM*, Paris, France, Apr. 2019.

[13] T.-J. Yang, Y.-H. Chen, and V. Sze, "Designing energy-efficient convolutional neural networks using energy-aware pruning," in *Proc. IEEE CVPR*, Honolulu, Hawaii, Jul. 2017.

[14] C. Louizos, K. Ullrich, and M. Welling, "Bayesian compression for deep learning," in *Proc. NeurIPS*, Long Beach, California, Dec. 2017.

[15] K. Yang, Y. Shi, W. Yu, and Z. Ding, "Energy-efficient processing and robust wireless cooperative transmission for edge inference," *arXiv preprint arXiv:1907.12475*, 2019.

[16] E. Basar, M. Di Renzo, J. De Rosny, M. Debbah, M. Alouini, and R. Zhang, "Wireless communications through reconfigurable intelligent surfaces," *IEEE Access*, vol. 7, pp. 116 753–116 773, Aug. 2019.

[17] M. Di Renzo, M. Debbah, D.-T. Phan-Huy, A. Zappone, M.-S. Alouini, C. Yuen, V. Sciancalepore, G. C. Alexandropoulos, J. Hoydis, H. Gacanin *et al.*, "Smart radio environments empowered by reconfigurable AI meta-surfaces: An idea whose time has come," *EURASIP J. Wireless Commu. Netw.*, vol. 2019, no. 1, pp. 1–20, Jan. 2019.

[18] C. Liaskos, S. Nie, A. Tsioliaridou, A. Pitsillides, S. Ioannidis, and I. Akyildiz, "A new wireless communication paradigm through software-controlled metasurfaces," *IEEE Commun. Mag.*, vol. 56, no. 9, pp. 162–169, Sept. 2018.

[19] Q. Wu and R. Zhang, "Intelligent reflecting surface enhanced wireless network via joint active and passive beamforming," *IEEE Trans. Wireless Commun.*, vol. 18, no. 11, pp. 5394–5409, Nov. 2019.

[20] C. Huang, A. Zappone, G. C. Alexandropoulos, M. Debbah, and C. Yuen, "Reconfigurable intelligent surfaces for energy efficiency in wireless communication," *IEEE Trans. Wireless Commun.*, vol. 18, no. 8, pp. 4157–4170, Aug. 2019.

[21] Q.-U.-A. Nadeem, A. Kammoun, A. Chaaban, M. Debbah, and M.-S. Alouini, "Asymptotic analysis of large intelligent surface assisted MIMO communication," *arXiv preprint arXiv:1903.08127*, 2019.

[22] C. Huang, S. Hu, G. C. Alexandropoulos, A. Zappone, C. Yuen, R. Zhang, M. D. Renzo, and M. Debbah, "Holographic MIMO surfaces for 6G wireless networks: Opportunities, challenges, and trends," *arXiv preprint arXiv:1911.12296*, 2019.

[23] H. Han, J. Zhao, D. Niyato, M. Di Renzo, and Q.-V. Pham, "Intelligent reflecting surface aided network: Power control for physical-layer broadcasting," *arXiv preprint arXiv:1910.14383*, 2019.

[24] M. Fu, Y. Zhou, and Y. Shi, "Intelligent reflecting surface for downlink non-orthogonal multiple access networks," in *in Proc. IEEE Globecom Workshops*, Waikoloa, Hawaii, Dec. 2019. [Online]. Available: https://arxiv.org/abs/1906.09434

[25] Y. Li, M. Jiang, Q. Zhang, and J. Qin, "Joint beamforming design in multi-cluster MISO NOMA intelligent reflecting surface-aided downlink communication networks," *arXiv preprint arXiv:1909.06972*, 2019.

[26] Q. Wu and R. Zhang, "Joint active and passive beamforming optimization for intelligent reflecting surface assisted SWIPT under QoS constraints," *arXiv preprint arXiv:1910.06220*, 2019.

[27] K. Li, M. Tao, and Z. Chen, "Exploiting computation replication for mobile edge computing: A fundamental computation-communication tradeoff study," *arXiv preprint arXiv:1903.10837*, 2019.

[28] Y. Mao, C. You, J. Zhang, K. Huang, and K. B. Letaief, "A survey on mobile edge computing: The communication perspective," *IEEE Commun. Surveys Tut.*, vol. 19, no. 4, pp. 2322–2358, Apr. 2017.

[29] A. Krizhevsky, I. Sutskever, and G. E. Hinton, "Imagenet classification with deep convolutional neural networks," in *Proc. NeurIPS*, Lake Tahoe, USA, Dec. 2012.

[30] D. Gesbert, S. Hanly, H. Huang, S. S. Shitz, O. Simeone, and W. Yu, "Multi-cell MIMO cooperative networks: A new look at interference," *IEEE J. Sel. Areas Commun.*, vol. 28, no. 9, pp. 1380–1408, Dec. 2010.

[31] T.-J. Yang, Y.-H. Chen, J. Emer, and V. Sze, "A method to estimate the energy consumption of deep neural networks," in *Proc. IEEE ACSSC*, California, USA, Oct. 2017.

[32] X. Xu, Y. Ding, S. X. Hu, M. Niemier, J. Cong, Y. Hu, and Y. Shi, "Scaling for edge inference of deep neural networks," *Nature Electronics*, vol. 1, no. 4, pp. 216–222, 2018.

[33] R. Mahapatra, Y. Nijsure, G. Kaddoum, N. U. Hassan, and C. Yuen, "Energy efficiency tradeoff mechanism towards wireless green communication: A survey," *IEEE Commun. Surveys Tuts.*, vol. 18, no. 1, pp. 686–705, Jan. 2015.

[34] "CNN Energy Estimation Website," http://energyestimation.mit.edu.

[35] Y.-H. Chen, T. Krishna, J. S. Emer, and V. Sze, "Eyeriss: An energy-efficient reconfigurable accelerator for deep convolutional neural networks," *IEEE J. Solid-State Circuits*, vol. 52, no. 1, pp. 127–138, Jan. 2016.

[36] I. Hwang, B. Song, and S. S. Soliman, "A holistic view on hyper-dense heterogeneous and small cell networks," *IEEE Commun. Mag.*, vol. 51, no. 6, pp. 20–27, Jun. 2013.

[37] M. Hong, M. Razaviyayn, Z.-Q. Luo, and J.-S. Pang, "A unified algorithmic framework for block-structured optimization involving big data: With applications in machine learning and signal processing," *IEEE Signal Process. Mag.*, vol. 33, no. 1, pp. 57–77, Jan. 2016.

[38] A. Wiesel, Y. C. Eldar, and S. Shamai, "Linear precoding via conic optimization for fixed MIMO receivers," *IEEE Trans. Signal Process.*, vol. 54, no. 1, pp. 161–176, Jan. 2006.

[39] M. Grant and S. Boyd, "CVX: Matlab software for disciplined convex programming, version 2.1," http://cvxr.com/cvx, 2014.

[40] S. Luo, R. Zhang, and T. J. Lim, "Downlink and uplink energy minimization through user association and beamforming in C-RAN," *IEEE Trans. Wireless Commun.*, vol. 14, no. 1, pp. 494–508, Jan. 2015.

[41] H. Dahrouj and W. Yu, "Coordinated beamforming for the multicell multi-antenna wireless system," *IEEE Trans. Wireless Commun.*, vol. 9, no. 5, pp. 1748–1759, May 2010.

[42] F. Bach, R. Jenatton, J. Mairal, G. Obozinski *et al.*, "Optimization with sparsity-inducing penalties," *Foundations Trends Mach. Learning*, vol. 4, no. 1, pp. 1–106, 2012.

[43] S. Boyd and L. Vandenberghe, *Convex optimization*. Cambridge University Press, 2004.

[44] Z.-Q. Luo, W.-K. Ma, M.-C. So, Y. Ye, and S. Zhang, "Semidefinite relaxation of quadratic optimization problems and applications," *IEEE Signal Process. Mag.*, vol. 27, no. 3, pp. 20–34, May 2010.

[45] T. Jiang and Y. Shi, "Over-the-air computation via intelligent reflecting surfaces," in *Proc. IEEE Globecom Workshops*, Waikoloa, Hawaii, Dec. 2019. [Online]. Available: https://arxiv.org/abs/1904.12475

[46] K. Yang, T. Jiang, Y. Shi, and Z. Ding, "Federated learning via over-the-air computation," *IEEE Trans. Wireless Commun., early access*, 2019.

[47] P. D. Tao and L. T. H. An, "Convex analysis approach to DC programming: theory, algorithms and applications," *Acta mathematica vietnamica*, vol. 22, no. 1, pp. 289–355, Jan. 1997.

[48] J. D. Griffin and G. D. Durgin, "Complete link budgets for backscatter-radio and RFID systems," *IEEE Antennas and Propagation Mag.*, vol. 51, no. 2, pp. 11–25, Apr. 2009.